Design of a Micro-Turbine for Energy Scavenging from a Gas Turbine Engine

A Major Qualifying Project Report:

Submitted to the Faculty of

WORCESTER POLYTECHINC INSTITUTE

in partial fulfillment of the requirements for the

Degree of Bachelor of Science

By

Amanda Kalish

Elyssa Morrow

Michael Powers

Stephen Rose

Professor D.J. Olinger, Advisor

ABSTRACT

The testing of gas turbine engines is very important in determining engine performance and efficiency. Sensors such as temperature thermocouples and pressure transducers allow engineers to assess how the engine performs during evaluation test phases. Over 3500 sensors can be used on a single engine during one evaluation and certification phase. The wiring of these sensors can take much time, manpower, and money. The gas turbine energy industry is looking to use wireless sensors as a way of cutting time and money during engine tests while still maintaining the reliability of the sensors, however a method must be found to power these sensors.

This project investigates the design, fabrication, and testing of a micro-turbine system to be placed into the fan flow of the gas turbine engine in order to scavenge energy from the flow to power wireless sensors. Design constraints include the requirement that the micro-turbine system produce 5-10 Watts of power, fit within a 7.5 x 7.5 x 2.5 cm volume, and be able to withstand temperatures in the gas turbine fan flow. A literature review was conducted on existing micro-turbine systems in addition to other possible energy scavenging methods.

Wind velocities in the fan flow of a gas turbine engine typically range from Mach 0.2 (68 m/s) to Mach 0.8 (272 m/s). In our proposed design, a portion of the fan flow is directed through an L-shaped tube to a micro-turbine connected to an electric micro-motor located outside of the engine. Basic kinetic energy and flow calculations predict that there will be enough kinetic energy in the flow at the end of the L-shaped tube to produce the 5-10 watts required to power the sensors. The micro-turbine is to be an axial turbine placed at the end of the L-shaped tube. Three turbine prototypes constructed with ABS plastic were 0.75 inches in diameter and ranged from 0.25 to 0.75 inches long, and were fabricated with a 3D printing technology. After initial testing with the

first iteration designs, blade aerodynamic theory was applied for second and third iterations in order to obtain an optimized micro-turbine design.

Using a compressed air source to mimic the fan flow, and a 9V electric micro-motor, three micro-turbine prototypes were tested experimentally. It was demonstrated that the most optimum design could produce 0.25 watts for an expected sensor resistance of 100 ohms at a fan flow velocity of approximately 200 m/sec. A maximum power of 1.4 watts was demonstrated for a sensor resistor of 10 ohms.

ACKNOWLEDGEMENTS

We would like to acknowledge and thank:

Justin Urban at Pratt and Whitney;

Professor D.J Olinger at Worcester Polytechnic Institute;

WPI Physics Department for the use of their strobe light.

Thank you for your guidance and assistance with this project.

TABLE OF CONTENTS

LIST OF FIGURES

1. INTRODUCTION

The testing of gas turbine engines is very important to verify that the engine is working correctly and efficiently. Sensors on the engine measure variables such as temperature and pressure. With these sensors, engineers can assess how the engine performs during the evaluation test phases. These sensors, such as thermocouples, are crucial in identifying any problems in the performance before the engine is shipped to the customer.

Since these sensors are so important, there can be over 3500 of them on the engine during one evaluation and certification phase (DeAnna, 2000). The wiring of these sensors can take much time and manpower as well as cost money. The gas turbine engine industry is looking to move to wireless sensors as a way of cutting time and money while still maintaining the reliability of the sensors. At Pratt and Whitney, engineers would like to use wireless sensors during test phases but realize that there needs to be a way to get power to the many sensors on the engine.

One of the obvious choices for power is batteries. While these are cheap and easy to acquire, they may not last the length of test. Testing can last over 1,000 hours and most batteries would need to be replaced before testing is complete. The replacement of these sensor batteries would create much battery waste and therefore creating an environmental concern. In addition, some sensors are deep inside the engine and parts of the engine may need to be disassembled in order to replace some of these batteries. Other ways to scavenge energy from the engine include thermal energy, vibrational energy and wind energy. In 2007, a team from Worcester Polytechnic Institute (WPI) researched thermal energy scavenging and built a thermoelectric generator package. This generator used the temperature difference between the ambient air and station 12.5 at the gas turbine engine to generate power (Bradway, et al, 2008).

This project will investigate another energy scavenging method by placing a micro-turbine placed in the gas turbine fan flow. A micro-turbine would need to be capable of producing enough wattage to power wireless sensors for engine testing. Research will be conducted on any existing energy scavenging involving wind powered micro-turbines. This project will involve the design and construction of an energy scavenging package using a micro-turbine that can produce between 5 and 10 watts of power. Justin Urban, an engineering fellow and project liaison from Pratt and Whitney, has stated that the final micro-turbine package should be no larger than 1x1x3 inches.
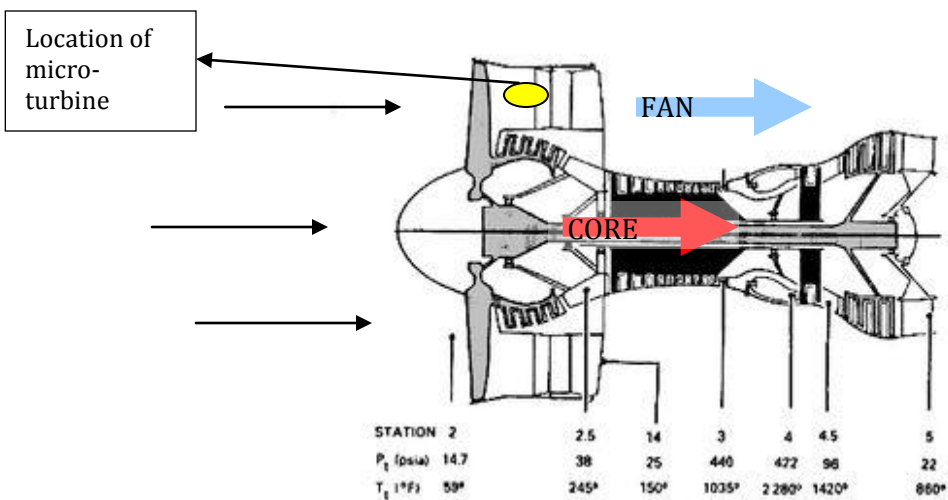
FIGURE 1- DIAGRAM OF GAS TURBINE ENGINE
HTTP://WEB.MIT.EDU/16.UNIFIED/WWW/SPRING/PROPULSION/NOTES/NODE27.HTML

2. BACKGROUND

A literature review was conducted on possible energy scavenging methods. A review of similar research and previous work was also conducted on micro-turbines in gas turbine engines.

2.1 CURRENT ENERGY SCAVENGING METHODS

There is currently a wide range of applications for wireless sensor networks. For different applications, different energy scavenging methods can be used. Possible power sources can come

from batteries, air/wind flow, solar, temperature, human power and vibrations. Figure 2 displays different types of power sources and their possible contribution.

Table –1.5. Comparison of various potential power sources for wireless sensor networks. Values shown are actual demonstrated numbers except in two cases, which have been italicized.

Power Source	P/cm³ (μW/cm³)	E/cm³ (J/cm³)	P/cm³/yr (μW/cm³/yr)	Secondary storage needed	Voltage regulation needed	Commercially available
Primary Battery	-	2880	90	No	No	Yes
Secondary Battery	-	1080	34	-	No	Yes
Micro-fuel cell	-	3500	110	Maybe	Maybe	No
Ultra-capacitor	-	50–100	1.6 – 3.2	No	Yes	Yes
Heat engine	-	3346	106	Yes	Yes	No
Radioactive (^{63}Ni)	0.52	1640	0.52	Yes	Yes	No
Solar (outside)	15000 *	-	-	Usually	Maybe	Yes
Solar (inside)	10 *	-	-	Usually	Maybe	Yes
Temperature	40 * †	-	-	Usually	Maybe	Soon
Human Power	330	-	-	Yes	Yes	No
Air flow	380 ††	-	-	Yes	Yes	No
Pressure Variations	17 †††	-	-	Yes	Yes	No
Vibrations	300	-	-	Yes	Yes	No

* Denotes sources whose fundamental metric is power per *square* centimeter rather than power per *cubic* centimeter.
† Demonstrated from a 5 °C temperature differential.
†† Assumes air velocity of 5 m/s and 5 % conversion efficiency.
††† Based on a 1 cm³ closed volume of helium undergoing a 10 °C temperature change once per day.

FIGURE 2-COMPARISON OF POTENTIAL POWER SOURCES (ROUNDY, 2004)

2.1.1 BATTERIES

Batteries are relatively inexpensive and can be disposed and replaced easily. Batteries might work for other wireless sensor networks but they are not the ideal choice for sensor power on gas turbine engines. Batteries lose charge over time, which is not ideal since an engine may sit wired up for weeks or months before being tested. The batteries must also last the full duration of all tests as some last up to 1000's of hours. Replacing batteries can require much work, or in some cases, disassembling areas of the gas turbine engine to access the battery locations. Batteries can also cause an environmental problem. Disposing of hundreds of batteries can leak lead and acid into the ground and water and also cause danger to human skin tissue (Environmental Hazard of Batteries, 2006).

2.1.2 THERMAL ENERGY

Thermal energy can be generated by differences in temperatures between two surfaces by thermo-electric devices. The most common way to generate power from differences in temperature is through a thermoelectric or piezoelectric generator (Roundy, 2004). Equation 1 shows the maximum efficiency of a thermal energy device. In general, the greater difference in temperature, the more power the system can produce.

$$\eta = \frac{T_{high} - T_{low}}{T_{high}} \tag{1}$$

In 2007-2008 a project group from WPI utilized the temperature difference between engine station 12.5 and the ambient air surfaces to generate a small voltage. By using a thermoelectric generator, 2.5 volts was generated for a temperature difference of 60°C. The device was set in between two metal plates with a heat sink. Batteries were used to help the device during engine start up (Bradway, et al, 2008). This device met the stated design requirements for the project, but was never tested in the engine.

2.1.3 VIBRATIONAL ENERGY

Vibrational energy is not available to all wireless sensor networks due to some systems not having any vibrations to work with. Gas turbines vibrate so this is a possible energy source. Some other examples of systems where vibrational energy scavenging could be used would be on machine shop tools, and kitchen appliances. Possible ways to convert vibrational energy into electric include the use of piezoelectric, electrostatic and electromagnetic generators. S. Roundy and colleagues developed a piezoelectric generator that used vibrational energy to generate

approximately 100 µW (Roundy, 2004). Equation 2 describes the power output from vibrations where "*P* is the power output, *m* is the oscillating proof mass, *A* is the acceleration magnitude of the input vibrations, ω is the frequency of the driving vibrations, ζ*m* is the mechanical damping ratio, and ζ*e* is an electrically induced damping ratio" (Roundy, 2004).

$$P = \frac{m\zeta_e A^2}{4\omega(\zeta_e + \zeta_m)^2} \qquad (2)$$

Vibrational energy can be used on a gas turbine engine but it would need to be a secondary source of power. As stated before, 5-10 watts of power need to be created and a very small piezoelectric generator that would fit in the specified size requirement would not create that amount of power.

2.1.4 HUMAN POWER

Although human power is not very practical for the application of a gas turbine engine, there is research being conducted on scavenging energy using human work. One research group at MIT has created a magnetic shoe generator that attaches to your shoe or sneaker and can create enough power to run a small radio (Paradiso, 2005). Other examples of human input in energy scavenging are magnetic generator flashlights and wind up radios.

2.1.5 TURBOCHARGERS

Turbochargers are small fan pumps that are run by the exhaust fumes of an engine and can range in size from 1.25in to 5in in diameter. They include a turbine and a compressor that are connected to each other through a shared axle. The exhaust fumes from the engine go through the

turbine and this in turn powers the compressor. Its purpose is to use exhaust air in order to increase power output (Nice, 2000)

Some turbochargers are fairly small and parts from them could be used in our micro-turbine device. Although the smallest car turbocharger has a turbine diameter of 1.25 inches, there may be ways to reduce the diameter.

2.1.6 WIND AND AIR POWER

Wind power is becoming quite popular as an alternative source of energy. Many wind farms are springing up across the nation and the world. The large wind turbines that are very well known today can have up to 40% efficiency while smaller scale versions can operate at efficiencies up to 20% (Roundy, 2004). There are various sizes and designs of wind turbine blades and systems in order to optimize the amount of power gathered from the wind. Optimum designs features include a high RPM motor and the use of a gearbox (Thomas, 2005)

Wind energy is a good way to power wireless sensors on a gas turbine engine. Speeds in the fan flow of the engine can reach up to Mach 0.8 which could create a sufficient amount of power.

2.2 PREVIOUS WORK ON ENERGY SCAVENGING WITH MICRO-TURBINES

Limited work has been done with micro-turbines in an energy scavenging application. A miniature turbine was developed by the Micro and Precision Engineering Group at Katholieke Universiteit Leuven in 2005. It was tested with compressed air at 330°C (626°F) and produced 130,000 rpm. At 18% efficiency it outputs approximately 28 Watts of power. The air enters through a pneumatic connector and travels through a stationary nozzle as seen in figure 3. The

nozzle deflects the air so that it hits the turbine blades tangentially. The air then leaves through the outlet disc (Micro and Precision Engineering Research Group, 2005).

All of the parts except for the connector and the circlip are stainless steel. The turbine has a diameter of 10mm (0.394in) and the housing has a diameter of 15mm (0.591in) and a length of 25mm (0.984in) (Micro and Precision Engineering Research Group, 2005).
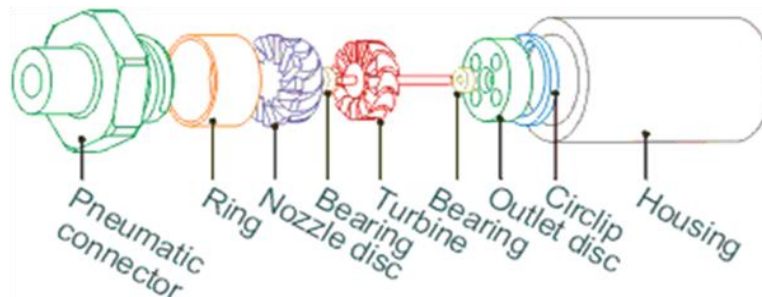
FIGURE 3- MICRO-TURBINE DESIGN (MICRO AND PRECISION ENGINEERING RESEARCH GROUP, 2005)

Pratt and Whitney is very interested in this design. The Micro and Precision Engineering Research Group was contacted about their design and the possibility of selling it. The research group had made three of them, one which was sold to a company. They had no interest in selling to students but gave some tips on how to make one. The machines they suggested to make it are not available at WPI.

2.3 PROJECT OBJECTIVES

This projects aims to satisfy the following objectives:

- Research existing energy scavenging methods including air powered micro-turbines.
- Estimate power available from a micro-turbine versus extraction pipe size, Mach number and pressure ratio.

- Design, test and optimize a micro- turbine system in order to extract 5-10 watts of power and meet the optimum size requirement of 1x1x3 inches.

The first objective will be accomplished by acquiring articles dealing with energy scavenging. If a design such as one listed above already exists, we will contact the designers and see about purchasing some. The second and third objectives will be completed by computing theoretical power numbers, and then experimentally testing different turbine designs. Once a first round of testing has been completed, optimization of the turbine will take place in order to re-design the turbine.

3. DESIGN OF ENERGY SCAVENGING SYSTEM

The design of the energy scavenging system has requirements including a maximum size and minimum power output. This section covers the steps taken in order to develop a system to meet the following requirements:

- Extract 5-10 watts of power

- Optimum size of micro-turbine package in Figure 4 to be 1x1x3 inches

- Withstand temperatures of 130ºF (DeAnna,2000)

This package will sit outside the engine. The package must be small because there is not a lot of space for the package in the area of interest on the engine.

3.1 SCHEMATIC OF FAN FLOW AND MICRO-TURBINE SETUP
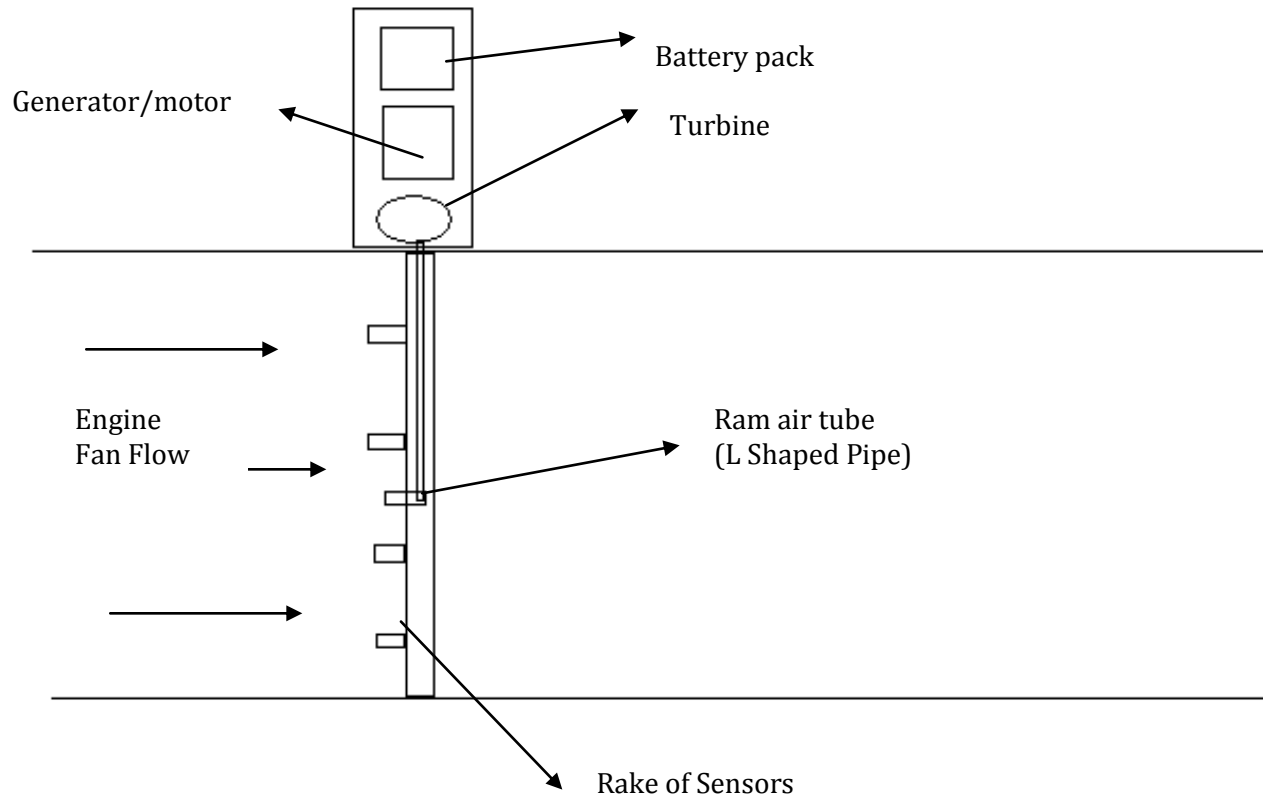
FIGURE 4- ENGINE AND MICRO-TURBINE PACKAGE SCHEMATIC

A current gas turbine engine test stand uses a rake of sensors in the fan flow at station 12.5. Each of the sensors is wired to an external power source. With multiple sensors per rakes and the wiring can become quite cumbersome.

The air from the fan flow goes past a rake of sensors. A L-shaped pipe will be incorporated into the rake in order to direct air from the fan flow to the micro-turbine package. Once the air hits the turbine, the turbine will spin and create mechanical energy which will be converted to electrical power by a generator. The generator will be attached to a battery pack which will then power the wireless sensors.

3.2 CALCULATIONS FOR ELECTRICAL POWER OUTPUT

Power calculations were conducted to estimate the amount of power that could be obtained from the environment in the fan flow of the engine. Basic calculations involving no frictional losses were done prior to calculations with losses due to friction and bends in the pipe.

3.2.1 BASIC POWER (KINETIC, NO LOSSES)

Basic power calculations were done in order to obtain a general idea on how much available power was available in the fan flow. These calculations were based on diameter of L-shaped pipe and speed in fan flow. In equation 3, ρ is the air density V is the air velocity at station 12.5 and A is the area of the L shaped pipe. The density will be considered constant due to the low flow velocities available, and will be the standard air density at sea level.

$$Power = \rho_{air} V_{FAN}{}^3 A_{PIPE} / 2 \qquad (3)$$

Power was calculated for a L-shaped pipe with a diameter of ¼ inch. We varied the velocities between Mach 0.2 (68 m/s) and Mach 0.8 (272 m/s) as specified by Justin Urban at Pratt and Whitney.

This calculation assumes an ideal flow with no losses in the L-shaped pipe so that the Vfan=Vexit where Vexit is the flow velocity spinning the turbine at the end of the L-shaped pipe. Later, calculations will include losses in the L-shaped pipe. Figure 5 below shows the control volume used in this equation.
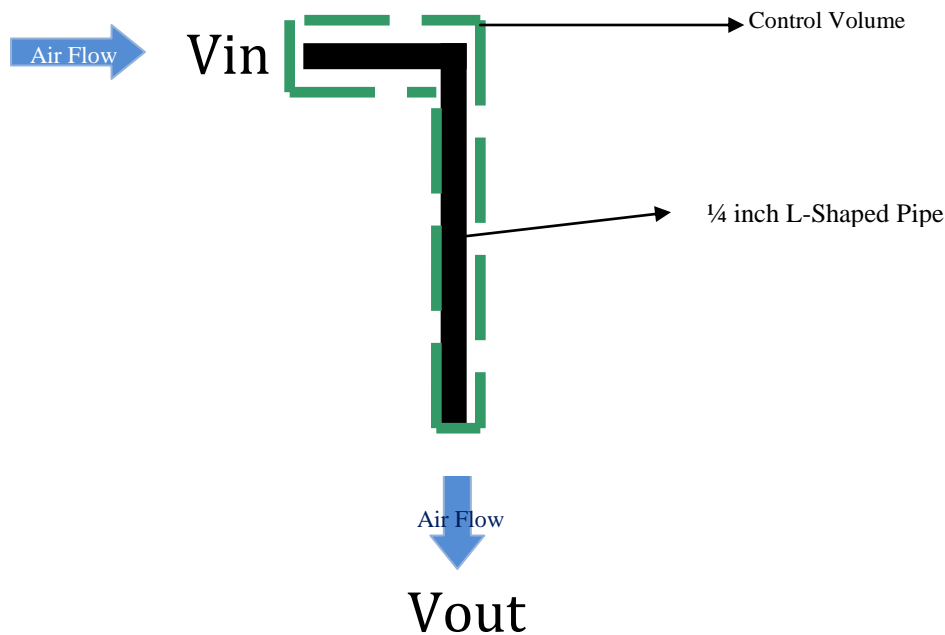
FIGURE 5- CONTROL VOLUME BASIC POWER CALCULATION

Since losses are expected during conversion between mechanical and electrical power, an efficiency term was added to these calculations. We expect to have between 5-20% efficiency. Equation 4 shows how efficiency changes the power available. Efficiency at 5, 10 and 20 percent was calculated.

$$Power(available) = Eff * 0.5 * \rho_{air} V_{FAN}^{3} A_{PIPE} \qquad (4)$$

Figure 6 and 7 show the available power in the fan flow at different efficiencies.
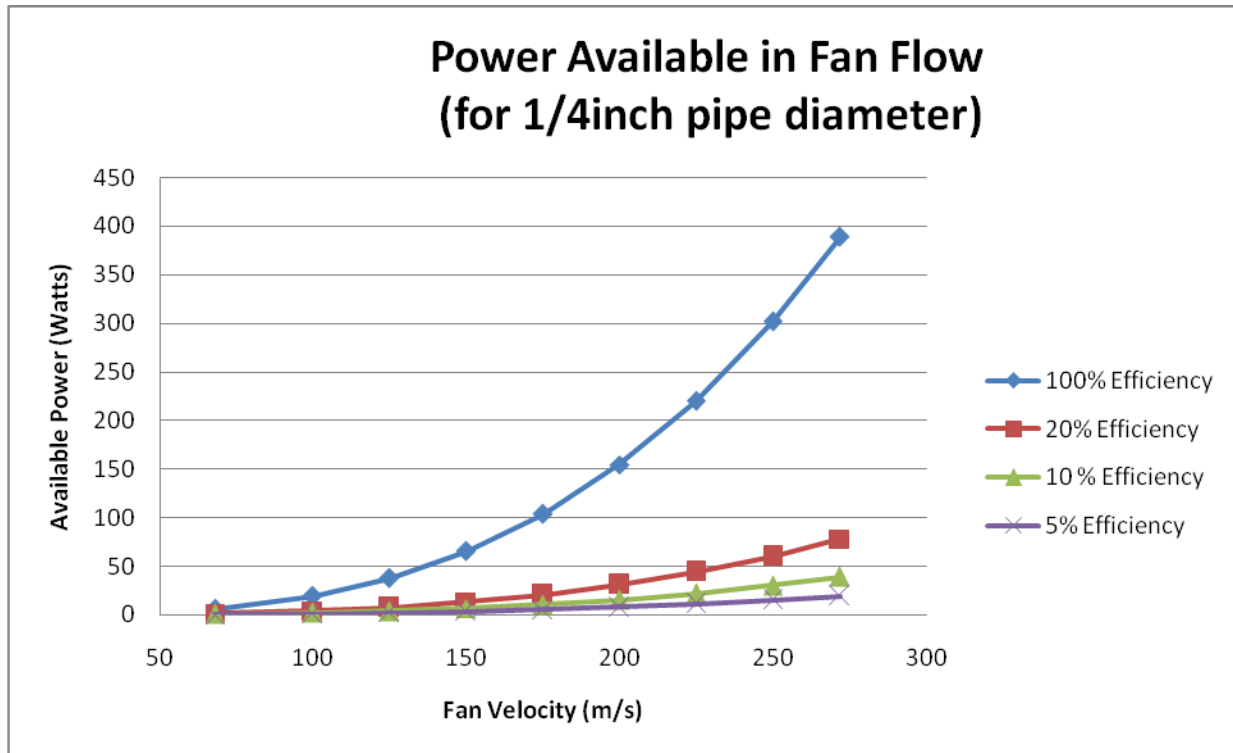
FIGURE 6- POWER AVAILABLE IN FAN FLOW FOR 1/4INCH PIPE
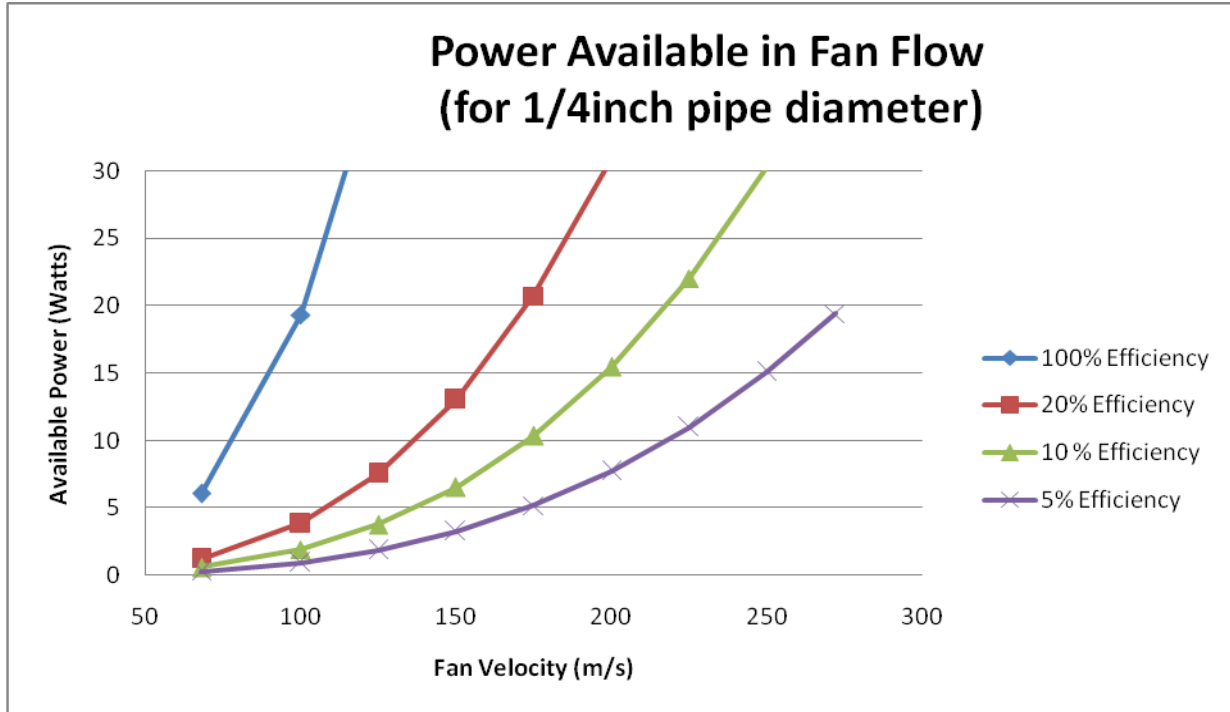
FIGURE 7- POWER AVAILABLE IN FAN FLOW FOR 1/4INCH PIPE (LOW POWER VALUES)

As shown, there is sufficient power available to meet the goal of 5-10 watts of power, but with low efficiencies, the amount of possible power is decreased.

Using equation 3 and 4 it is fairly simple to calculate the power that can be generated at different air velocities. Since the velocity of the fan flow varies along the engine, this will help determine where the generator must be placed.

3.2.2 BASIC POWER USING ENERGY EQUATION WITH DELTA PRESSURE TERM INCLUDED

The second round of calculations included losses in the pipe including friction. Minor and major losses as mentioned above were also included in that calculation. In addition, the control volume used is shown below in figure 8.
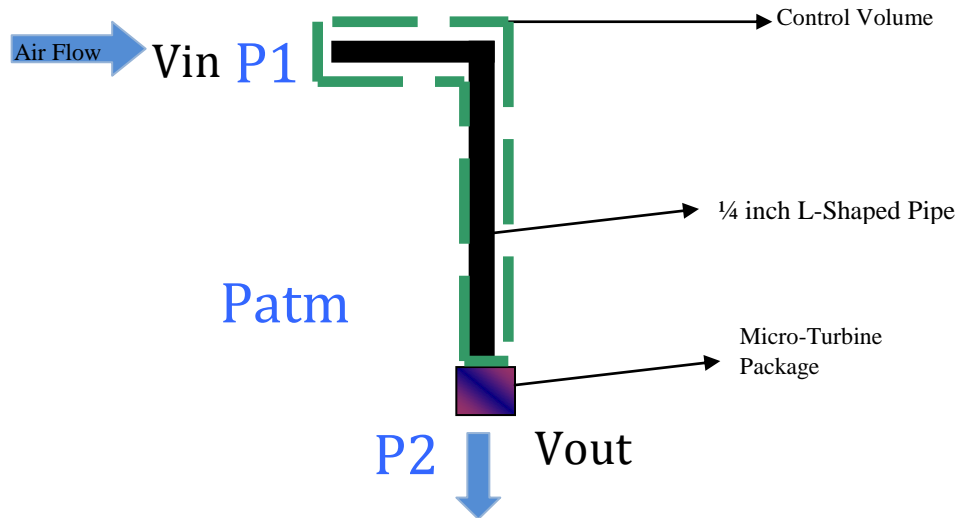
FIGURE 8-CONTROL VOLUME

The L shaped pipe is 3 feet long (l) and 1/4 inch diameter (D).

$$MajorLoss = f(\frac{l}{D})(\frac{V_{FAN}^2}{2}) \qquad (5)$$

$$MinorLoss = k(\frac{V_{FAN}^2}{2}) \qquad (6)$$

Minor losses include the 90 degree bend and inlet of the pipe. The frictional faction was determined by using a Moody chart (as shown in Figure 9) and the Reynolds number and relative roughness of the pipe. The friction factor, f, for the stainless steel pipe was estimated to be about .044.
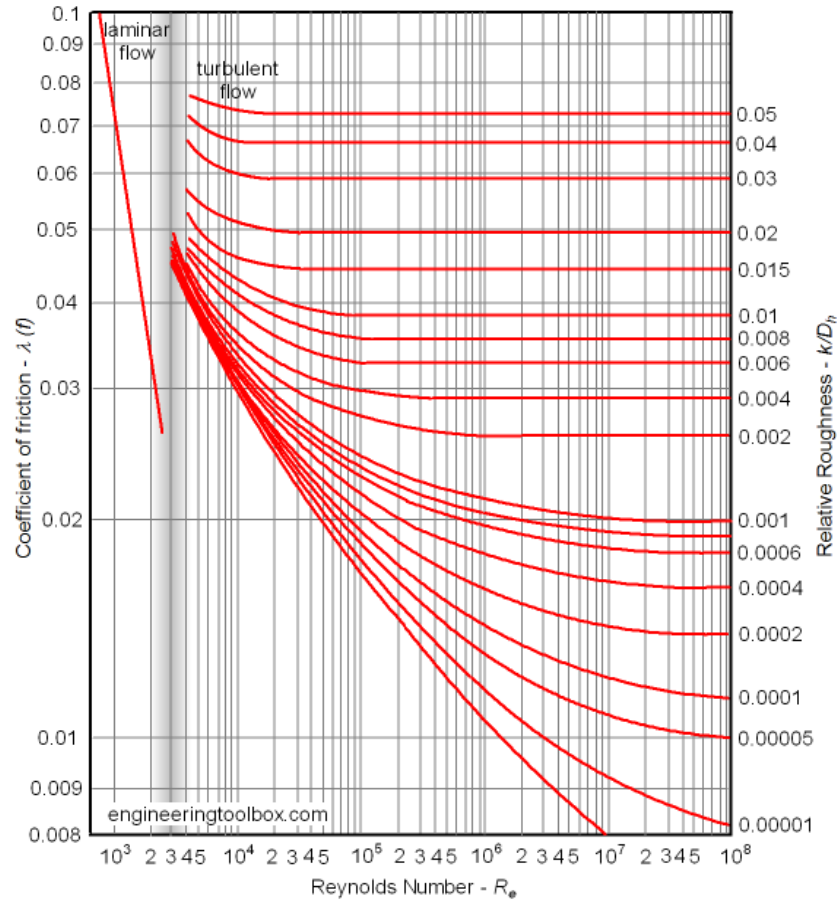
FIGURE 9-MOODY DIAGRAM
(WWW.ENGINEERINGTOOLBOX.COM)

By expanding on the energy equation to include the delta pressure term, the final equation

for total available power from fan flow is shown below in equation 7.

$$Power = \rho_{air}V_{FAN}{}^{3}A_{PIPE}/2 + V_{FAN}A_{pipe}(P_2 - P_{atm}) \qquad (7)$$

Where V is velocity in the Fan, A is area of the L shaped pipe. Delta P was calculated by

subtracting atmospheric pressure (Patm) from the pressure at the end of the pipe (P2). A fan

pressure ratio of 2 was assumed which sets P1=2 *Patm. P2 was calculated by equation 8.

$$P_2 = P_1 - f(\frac{l}{D})(\frac{V_{FAN}^2}{2}) - k(\frac{V_{FAN}^2}{2}) \qquad (8)$$

Figure 10 shows power calculations based on V in the fan flow. As shown by Figure 10, some of the delta pressures are negative; indicating that associated high velocity flows would not be possible at high speeds in small pipes.

Major Loses	Minor Losses	P1 (Pfan) (Pa)	P2 (pressure at end of L Shaped pipe) (Pa)	Patm (Pa)	A of pipe (m)	Vfan (compressed air) (m/s)	delta P (Pa)	V at Turbine (m/s)	Power Available (100% Eff.) (W)	15% Eff. (W)
14648.832	4207.84	202600	183743.328	101300	3.16692E-05	68	82443.328	39.2598183	103.6539047	15.54808571
17820	5118.75	202600	179661.25	101300	3.16692E-05	75	78361.25	43.30127019	109.000873	16.35013095
31680	9100	202600	161820	101300	3.16692E-05	100	60520	57.73502692	114.3130136	17.14695203
49500	14218.75	202600	138881.25	101300	3.16692E-05	125	37581.25	72.16878365	93.03531087	13.95529663
71280	20475	202600	110845	101300	3.16692E-05	150	9545	86.60254038	38.52030411	5.778045617
97020	27868.75	202600	77711.25	101300	3.16692E-05	175	-23588.75	101.0362971	-55.87946751	-8.381920126
126720	36400	202600	39480	101300	3.16692E-05	200	-61820	115.4700538	-196.8114648	-29.52171972
160380	46068.75	202600	-3848.75	101300	3.16692E-05	225	-105148.75	129.9038106	-390.9231486	-58.63847229
198000	56875	202600	-52275	101300	3.16692E-05	250	-153575	144.3375673	-644.8619797	-96.72929696
230947.2	66339	202600	-94686.2	101300	3.16692E-05	270	-195986.2	155.8845727	-895.5556843	-134.3333526

FIGURE 10-POWER CALCULATIONS WITH LOSSES-FAN PRESSURE RATIO OF 2

Velocity in Fan Flow vs Available power
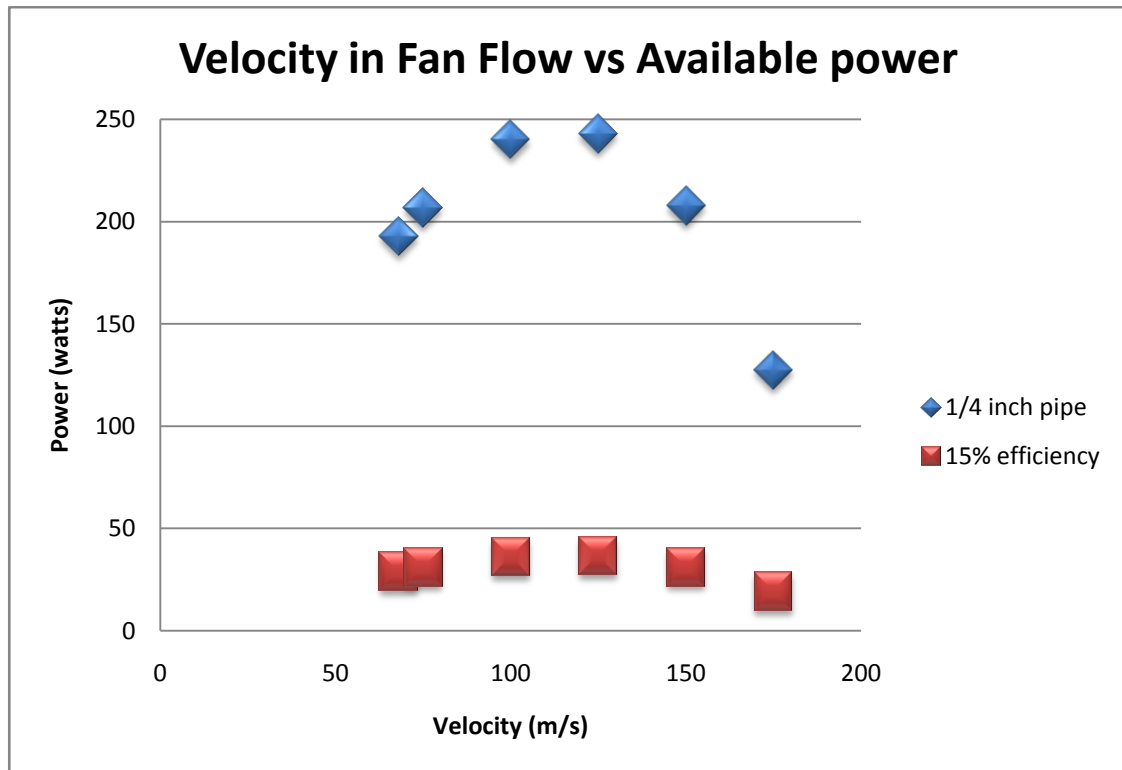
FIGURE 11-AVAILABLE POWER (LOSSES INCLUDED)

Figure 11 shows the plot of possible power output for 100% and 15% assumed efficiencies.

At 100m/s the power is at a maximum. This is most likely due to the small pipe diameter. The

flows at speeds higher than 100 m/s will experience too much turbulence and associated high

friction factors and viscous losses and will not be able to produce much power.

3.3 DESIGN OF MICRO-TURBINES

Three iterations of micro-turbines were made. This next section describes the design

process.

3.3.1 DESIGN OF FIRST ITERATION

This turbine relies on causing a maximum change in momentum to cause spin. Each blade wraps around the center of the turbine in a helical path. In this way they each perform a ninety degree twist around the turbine's center. This ninety degree rotation is intended to cause the maximum amount of tangential force to the turbine.

The sizing of this turbine was determined mostly from production limitations. As shown below in equation 9 for a given flow rate, $Q=V_1A_1$, the radius of the L-shaped pipe exit should be as small as possible in order to maximize the flow velocity at the turbine inlet.

$$P = \frac{\rho V_2^3 A_2}{2} \tag{9}$$

Here, P is the power available in the air flow, ρ is the density of air, V_2 is the compressed air velocity at the turbine and A_2 is the cross sectional flow area at the turbine. Equation 10 shows the conservation of mass equation.

$$\rho V_1 A_1 = \rho V_2 A_2 \tag{10}$$

Where V_1 is the compressed air velocity at the pipe inlet, and A_1 is the area of the pipe inlet. It is apparent that V_2 depends on V_1, so solving for V_2 and substituting into the first equation yields equation 11.

$$P = \frac{\rho V_1^3 A_1^3}{2A_2^2} \tag{11}$$

It is now obvious that in order to maximize power the cross sectional area, A_2 of the L shaped pipe exit must be as small as possible. The turbine should fit inside the L-shaped pipe in

order to eliminate losses, however due to manufacturing tolerances of the ABS plastic the smallest

turbine which could be made had a diameter of 0.75 inches. Therefore a nozzle was added to the

end of the L-shaped pipe to expand the exit area.

The turbine prototypes were designed using the computer aided design program, Solid

Works. The turbine design is a simple axial turbine. The dimensions can easily be modified to

change the sizing of the prototypes as the design evolves. The design, as shown in Figure 12,

measures .75 inches in diameter and .5 inch long.
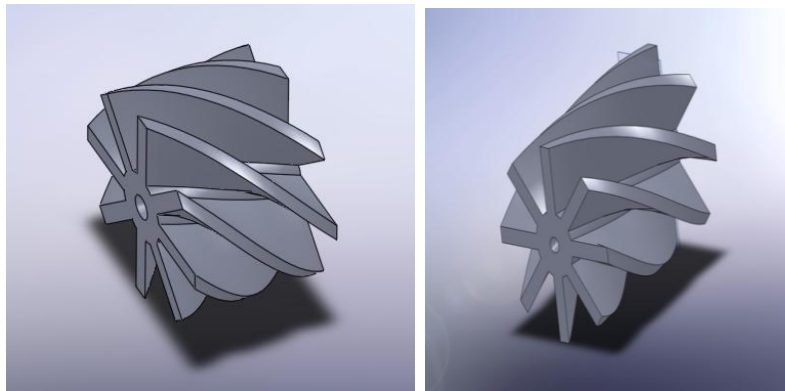
FIGURE 12- AXIAL TURBINE-FIRST ITERATION

The first prototypes were created in a Dimension SST AS rapid prototyping machine

available in the Mechanical Engineering Department at WPI. This machine creates the desired

prototype out of a CAD design by laying down thin layers of ABS plastic (acrylonitrile butadiene

styrene) until the entire structure is completed. This is the same type of plastic that Lego toys are

made out of. This method allows small parts to be created much more easily than a traditional

milling technique because its size is not limited by the available tool size. In this way prototypes

can be quickly and cheaply created as the design evolves.

After testing out the first iteration design, optimization was done in order to make a more efficient turbine.

3.3.2 DESIGN OF SECOND ITERATION

Determining the angle of the turbine blades was important in making an efficient turbine. The angle of the blades for this turbine was determined using velocity triangles and classic Euler turbo machinery equation for turbine blades. This concept uses the incoming air velocity and speed of the turbine blades to determine the angle of the blades.
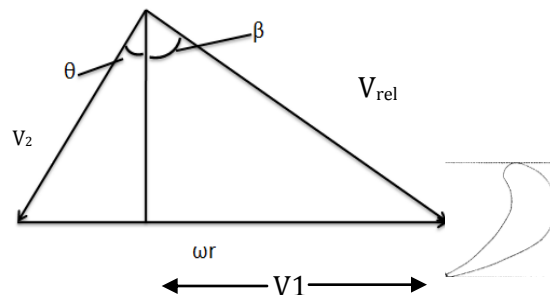
FIGURE 13: VELOCITY TRIANGLE AT TURBINE INLET

In Figure 13, ωr is the turbines' angular velocity multiplied by its radius, V_2 is the incoming compressed air velocity, V_{rel} is the velocity of the air relative to an observer on the turbine blade, θ is the angle of the incoming air velocity and β is the turbine blade angle.

A similar analysis can be performed at the turbine's exit. In this case, V_3 is the air velocity at the turbine exit, V_{rel2} is the velocity of the air relative to an observer on the turbine blade at the exit, θ is the angle of the air velocity within the turbine, and β remains the turbine blade angle.
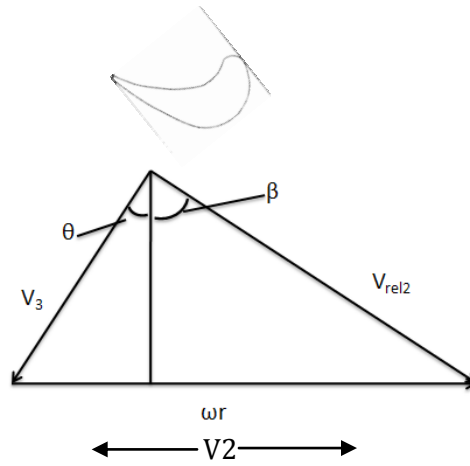
FIGURE 14: VELOCITY TRIANGLE AT TURBINE EXIT

For this application, the incoming compressed air velocity entering the turbine is perpendicular to the velocity of the turbine blades. This simplifies the velocity triangle as shown in Figure 15.
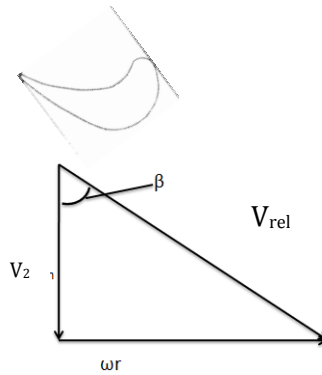
FIGURE 15: SIMPLIFIED VELOCITY TRIANGLE

From this the angle β, as shown in equation 12, can easily be determined from the known quantities, ωr and V_2.

$$\beta = tan^{-1}\left(\frac{\omega r}{V}\right)_{in}$$

(12)

V_2 was set to 200 m/s, which was the optimum velocity given for this application. An experimentally determined value of 628 1/s was set to ω, and a value of 0.375 in, or 0.953 cm, was used for the radius. The value of the radius is limited to this minimum value by the production

technique. This yields a blade angle of 1.69°. The final design for the second iteration turbine is shown in Figure 16.
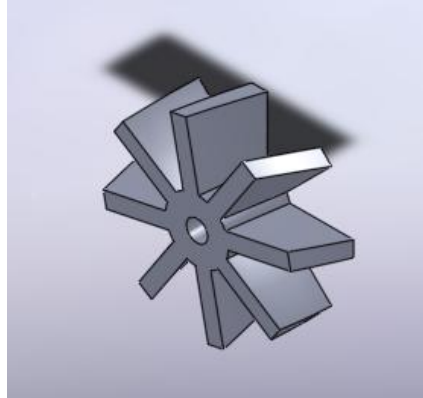
FIGURE 16: SECOND ITERATION TURBINE DESIGN

The turbine is .25 inches long and has a diameter of .75 inches. Figure 17 shows the turbine.
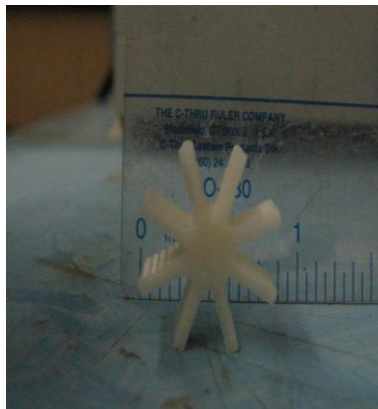
FIGURE 17-SECOND ITERATION TURBINE

3.3.3 DESIGN OF THIRD ITERATION TURBINE

The third iteration turbine was designed by treating the blades as a thin airfoil. It is known that the stall angle for a thin airfoil is approximately 10-15°, so this was used as the angle of attack for the flat blades. Figure 18 and Figure 21 show the final design of the third iteration turbine.
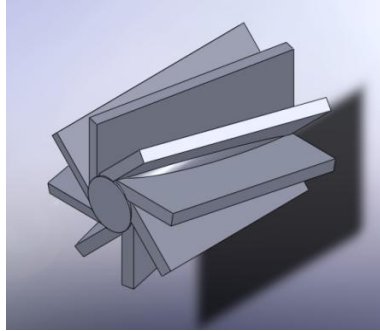
FIGURE 18: THIRD ITERATION TURBINE DESIGN

The power that can be generated from a turbine can be determined from the Euler turbine equation as shown in equation 13.

$$P = \rho V_1 A * \omega r (V_2 - V_1)$$ (13)

In equation 13, V_2 is the air velocity exiting the turbine blades and V_1 is the air velocity entering the turbine blades. V_1, however, acts perpendicular to the turbine and does not have an effect on power. It can therefore be ignored. The only component of V_2 which helps generate power is the component which lies perpendicular to the turbine. This velocity is shown in equation 14.

$$V_{2,perp.} = V_1 sin\theta$$ (14)

In equation 14, θ is the turbine blade angle. This leads to a final power equation shown in equation 15.

$$P = \rho V_1^2 A * \omega r sin\theta$$ (15)

If a value of 57 m/s is used for V_1 (approximately 100 m/s of fan flow) the power as a function of angle can be determined for any angle of attack up to the stall angle.

Angle (degrees)	Turbine Power (watts)	Angle (degrees)	Turbine Power (watts)

0	0	7	1.127659374
1	0.161487452	8	1.287771375
2	0.322925713	9	1.447491108
3	0.484265608	10	1.606769921
4	0.645457991	11	1.765559297
5	0.806453761	12	1.923810866
6	0.967203877		

FIGURE 19-THEORETICAL POWER FROM TURBINE ANGLES
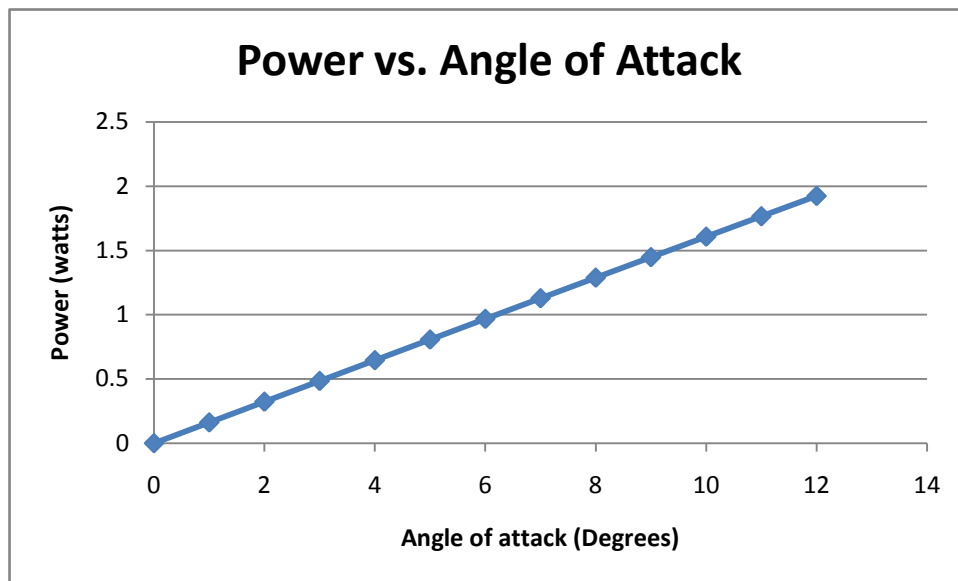
FIGURE 20-POWER VS. ANGLE OF ATTACK

As shown by Figure 19and Figure 20, the greater the angle of attack, the more power that can be generated. It is also clear that this type of turbine should be able to produce enough power to meet the design goals, but viscous losses and inefficiencies must still be taken into account.

The radius was once again made as small as was allowed by the tolerances of the production technique. The turbine diameter was once again .75 inches and the length was 1 inch. Figure 21 shows a picture of the turbine.
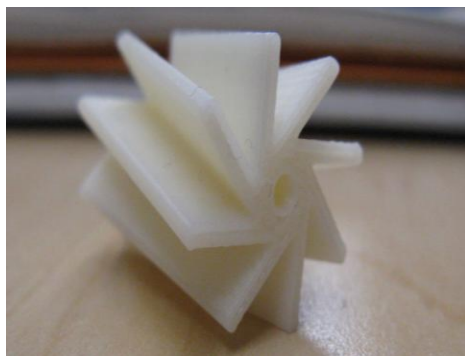
FIGURE 21- THIRD ITERATION TURBINE

3.4 DESIGN OF EXPERIMENTAL SETUP FOR ALL MICRO-TURBINE DESIGNS

This section explains the testing setup and experiments performed with the ¼ inch L-Shaped pipe and compressed air line.

3.4.1 DESIGN OF EXPERIMENTAL SETUP

In order to properly test our turbine design, a sturdy setup was needed. A compressed air jet was directed towards the ¼ inch diameter and 3 feet long L-shaped pipe. This length was chosen in order to approximate the length of the ram air pipe from the engine fan flow to the turbine housing. The inlet of the L-shaped pipe was placed 1 inch downstream from the compressed air jet outlet. The L-shaped pipe was placed in the centerline of the compressed air jet. The L-shaped pipe was bolted to a table and directed along to the turbine house. The turbine house was constructed of plywood with a moveable top so that modifications could be made. The intention of the turbine housing was safety. Within the turbine housing, the turbine was connected to the motor and then attached to another piece of plywood. From the motor, wires connected the turbine to a resistor and DAQ board to measure voltage and current. Figure 22 shows the experimental setup.
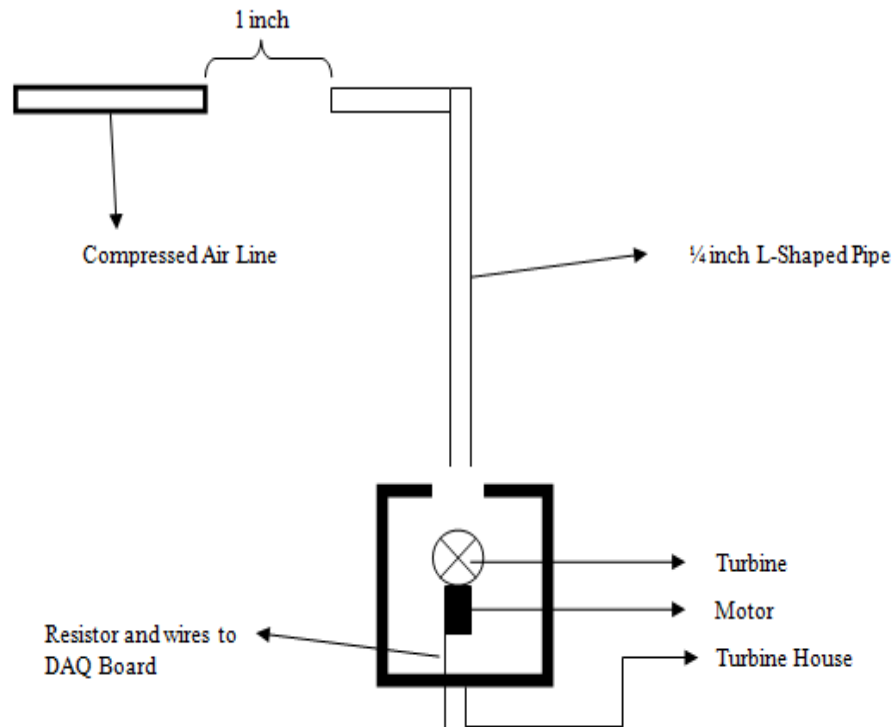
FIGURE 22-DRAWING OF TURBINE TEST SETUP

The setup was bolted to the table because the vibrations from the high compressed airspeeds caused vibration in the pipe as well as in the turbine/motor section. A wooden box was first used to contain the setup. It was later replace by a smaller lexan box. Figure 23-Figure 28 highlight the design of the housing and pipe.
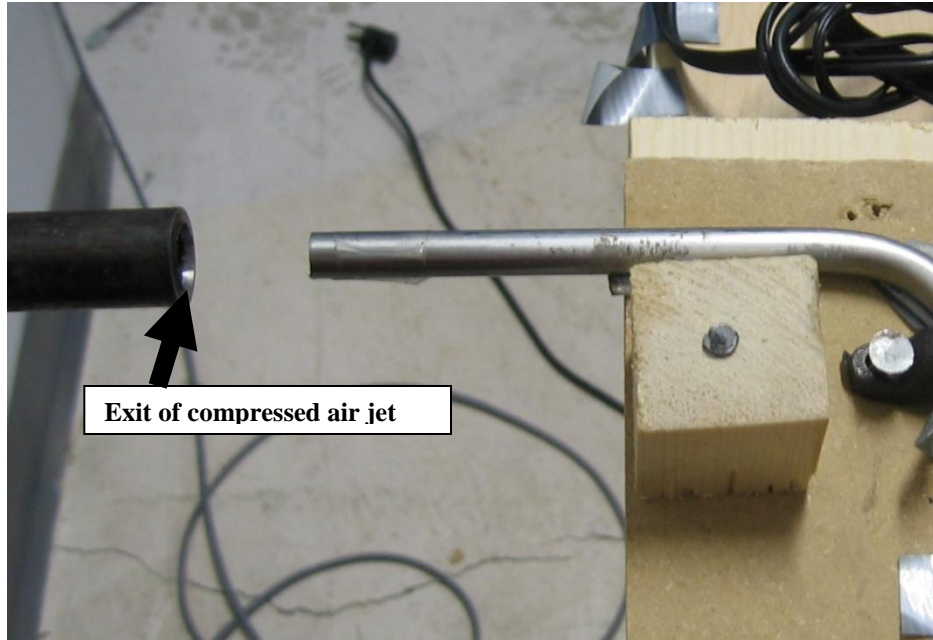
FIGURE 23-COMPRESSED AIR TO L-SHAPED PIPE

FIGURE 24 - INTAKE PIPE INTO TURBINE HOUSE

FIGURE 25 - EXIT OF TURBINE HOUSE

FIGURE 26 - TURBINE HOUSE VIEW 1
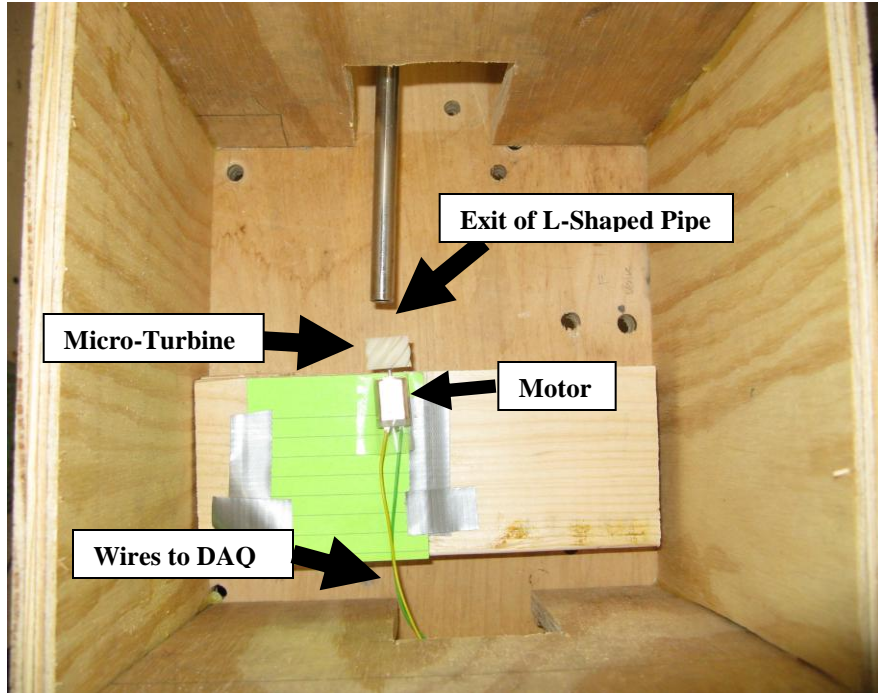
FIGURE 27 - TURBINE HOUSE VIEW 2

.
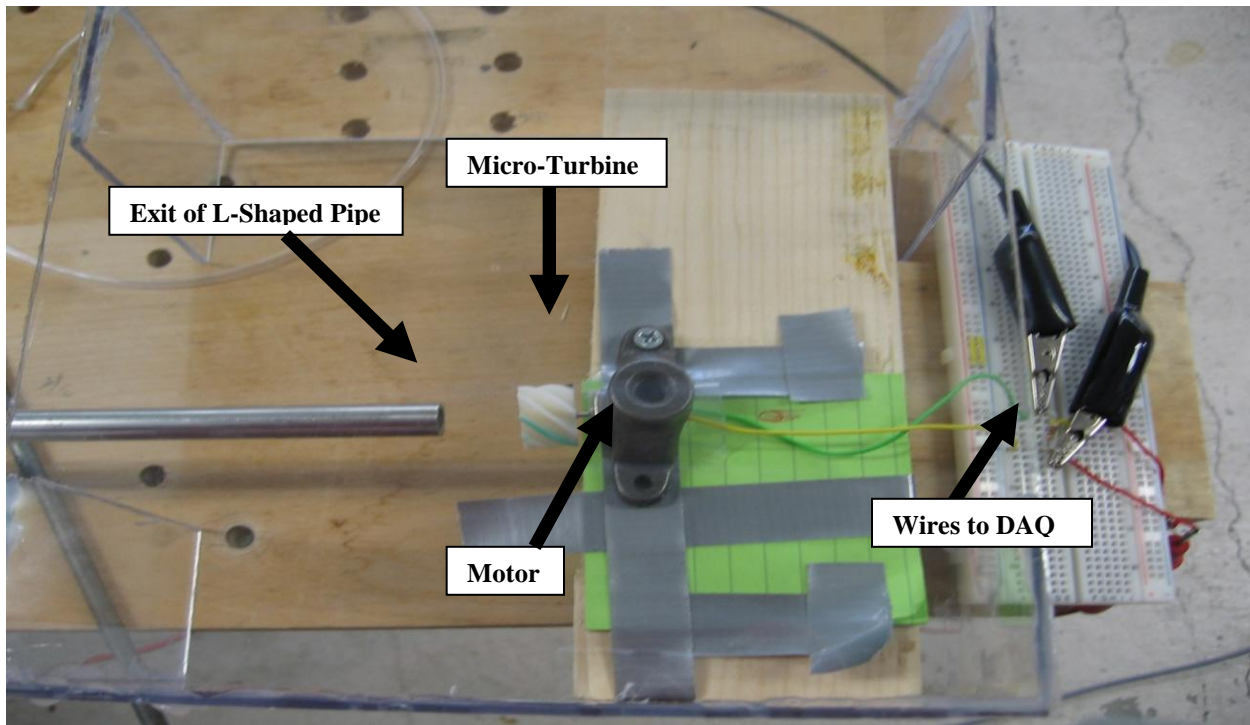
FIGURE 28 - EXIT OF L-SHAPED PIPE AND TURBINE

The following experimental setup is used to test the micro-turbine. This test must be done using compressed air since the correct type of flow cannot be achieved in a wind tunnel.

Using a compressed air line in WPI Higgins Labs 016 as pictured in Figure 29, it is possible to simulate the fan flow of a jet engine. The air must be compressed in order to properly simulate the fan flow. In a jet engine, the fan upstream pushes the air through the engine creating a higher than atmospheric pressure. A compressed air source creates the same high pressure but exhaust flow is still at atmospheric pressure.

FIGURE 29-MEASURING SPEED OF COMPRESSED AIR

It is important to know the velocity of the air in the compressed air jet, because this is the same velocity as the air going into the L-shaped pipe. In order to avoid blocking the flow a pitot probe was held 1 inch away from the compressed air jet. Since the air velocity varies in the direction perpendicular to the jet centerline, it is important to hold the pitot probe on the centerline of the jet in order to achieve the highest velocity and the most accurate results (Figure 30). The pitot probe is attached to a manometer or pressure transducer to measure the pressure difference between the airflow and the atmospheric pressure. The pressure transducer used was an Aerolab

force balance and pressure transducer. The velocity is determined be measuring the change in height of the water in the manometer or pressure transducer.
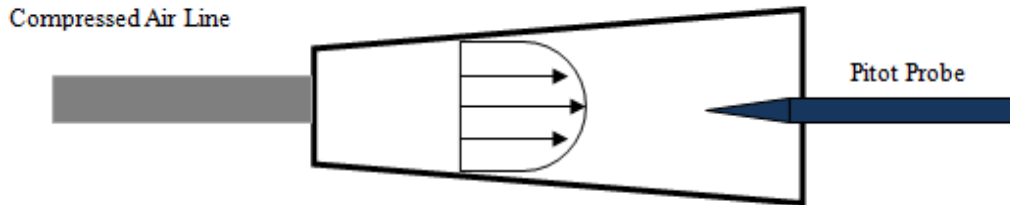
FIGURE 30- COMPRESSED AIR JET FLOW

Once there is an accurate velocity measurement, the L-shaped pipe can be placed into the flow as pictured in Figure 31. The front end of the L-shaped pipe must be placed exactly 1 inch from the compressed air source and must be parallel to the flow. This will allow for the maximum amount of air to enter the L-shaped pipe. In order to insure that the L-shaped pipe is correctly oriented, a wooden stand was built to hold it in place.
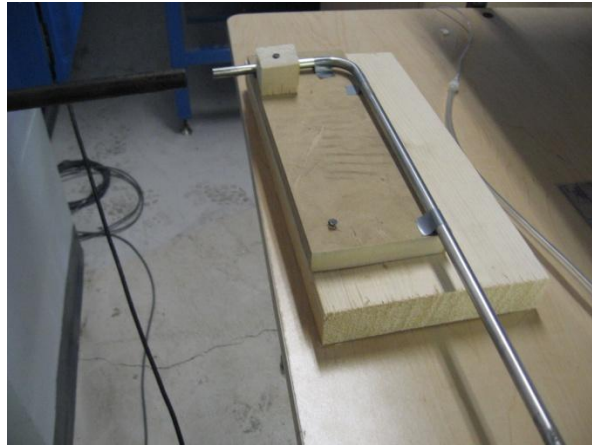
FIGURE 31- COMPRESSED AIR TEST SETUP

The velocity of the air exiting the L shaped pipe can be measured the same way as the velocity coming out of the compressed air source. Place a pitot probe directly into the airflow

coming out of the L-shaped pipe and measure the change in height of water in the manometer. The change in height of water, h, can then be used to calculate the air velocity, as given in Equation 16.

$$V_{compressed\ air} = \sqrt{\frac{2\rho_{H2O}gh}{\rho_{air}}} \tag{16}$$

The experiment described above should be repeated multiple times for different compressor velocities. Once a few data points have been obtained, it is possible to calculate the losses from the L-shaped pipe. This is achieved be calculating the ratio between the velocity of the air entering the L-shaped pipe and the velocity exiting it. Figure 32 shows the velocities at the entrance (inlet) and exit (outlet) of the L shaped pipe.

rho_H2O	998	kg/m^3
rho_air	1.2	kg/m^3
g	9.81	m/s^2

L-Shaped Pipe Inlet Velocities			L Shaped Pipe Exit Velocities			Ratio between Velocities
h (in)	h (m)	V (m/s)	h (in)	h (m)	V (m/s)	
1	0.0254	20.35828	0.3	0.00762	11.15069	0.547722558
2	0.0508	28.79095	0.6	0.01524	15.76945	0.547722558
4	0.1016	40.71655	1.2	0.03048	22.30137	0.547722558
6	0.1524	49.86739	1.8	0.04572	27.31349	0.547722558
7.5	0.1905	55.75344	2.2	0.05588	30.1962	0.54160256

FIGURE 32 - TABLE OF COMPRESSED AIR VELOCITIES AND L SHAPED PIPE EXIT VELOCITIES

As shown on the right, the experimentally determined ratio between inlet and exit velocities is approximately $1/\sqrt{3}$. Figure 33, below, compares the line y=x/sqrt(3) with the data points taken.
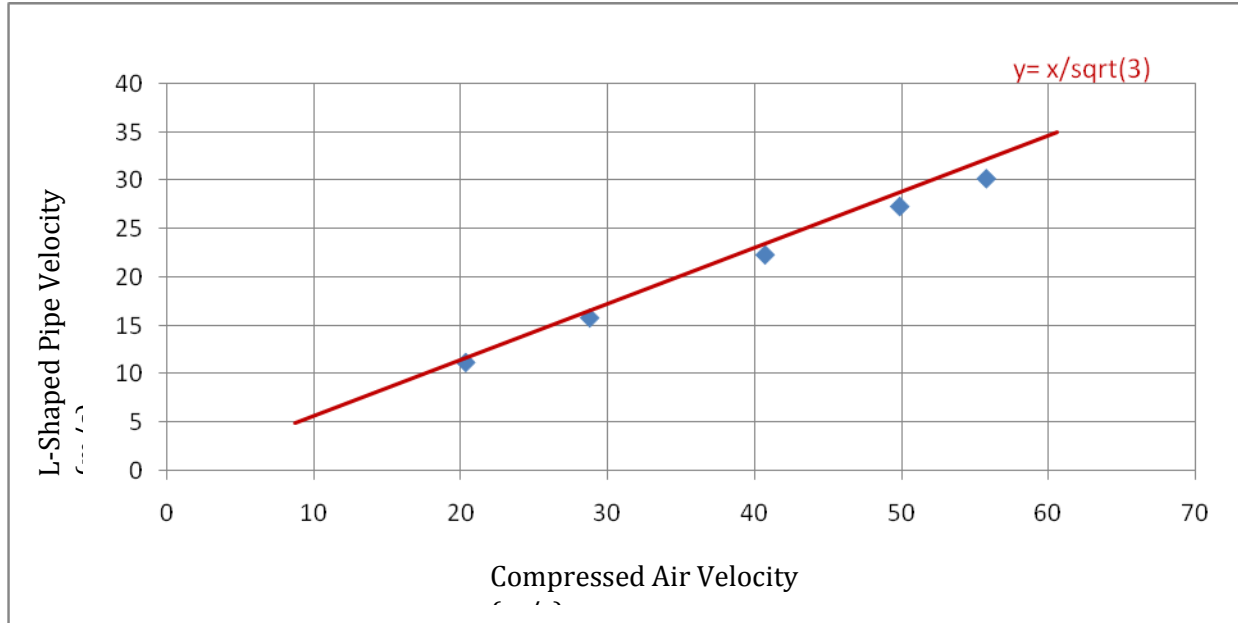
FIGURE 33 - COMPRESSED AIR VELOCITIES AND L SHAPED PIPE EXIT VELOCITIES RATIO

As mentioned above, a ratio of $1/\sqrt{3}$ between the velocities at the compressed air outlet and

L-Shaped Pipe outlet. Figure 34 shows the table of velocities at the compressed air outlet and L-

Shaped Pipe outlet.

V-Compressed air (m/s)	V-L Shaped Pipe Exit (m/s)
30	17.32051
45	25.98076
60	34.64102
90	51.96152
120	69.28203
150	86.60254
180	103.923
210	121.2436
240	138.5641
270	155.8846

FIGURE 34 - IDEAL INLET AND EXIT VELOCITIES

The final testing setup is show in Figure 35 and Figure 36. A strobe light was used to

calculate the RPM's of the turbines.
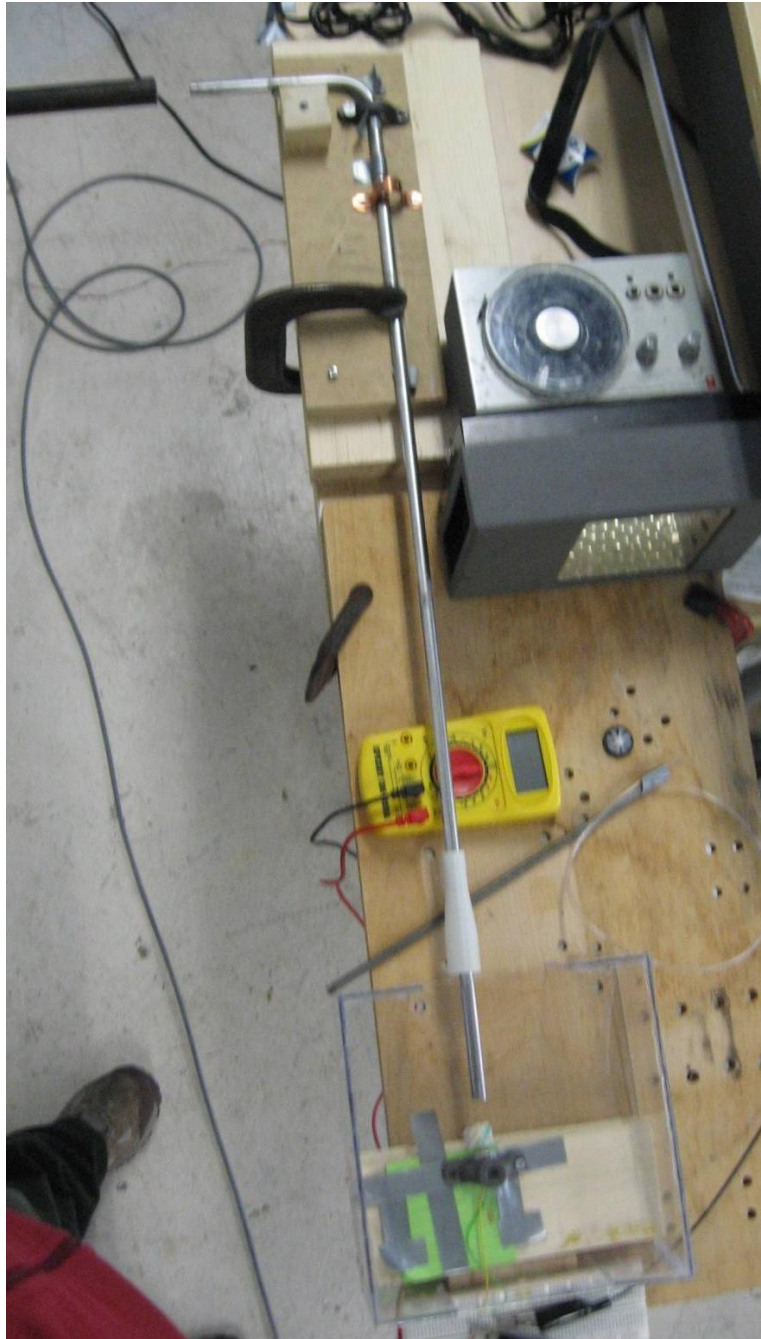
FIGURE 35-ENTIRE TEST SETUP

FIGURE 36- TURBINE WITH NOZZLE SETUP

4 TESTING AND RESULTS OF DIFFERENT MICRO-TURBINES

This section will detail the tests and results from testing different micro-turbines.

4.1 EXPERIMENTAL TESTING FIRST ITERATION DESIGN

The following section will describe the testing of the first iteration turbine design.

4.1.2 RESISTIVE LOAD TESTING

Power outputs were measured for the micro-turbine design using three different loads. Power is determined by measuring the voltage output for different compressed airspeeds and dividing that by the square of the load's resistance. Each point plotted uses the average of a few thousand measured voltages to determine the voltage output for a given compressed airspeed.

Initial tests show that the maximum achievable power with the first iteration turbine is approximately 0.25 Watts. The accuracy of these results is, however, questionable due to the fact

that the 10 ohm resistor produced the least power. In theory, power is equal to voltage squared divided by resistance. It is also true that voltage does not vary with resistance; it is strictly a function of turbine RPM, which is a function of compressed airspeed. Therefore, the 10 ohm resistor should produce 10 times more power than the 100 ohm resistor for a given compressed airspeed. This is clearly not the case, which suggests that there may be a loose connection in the setup. Figure 37 shows a plot of the power verses compressed airspeed.
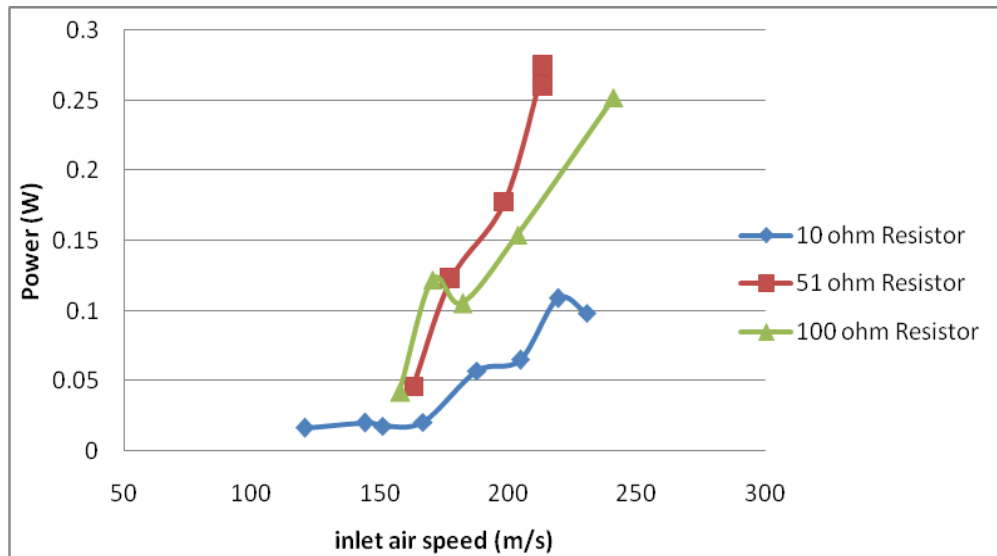
FIGURE 37-POWER OUTPUT VARYING WITH RESISTANCE

According to Justin Urban of Pratt and Whitney, the pressure transducer draws 10mA of current at a 10V excitation. According to equation 17, voltage equals current multiplied by resistance.

$$V = IR \qquad (17)$$

From this equation, resistance is found to be 1000 ohms. There are approximately 1o sensors in a rake and since these sensors are connected in parrallel, the resistance through each pressure sensor will be 100 ohms and will require .1 W of power.

4.1.3 NO LOAD TESTING

Once it was discovered that the breadboard setup, including the resistor, was effecting measurements, all following voltage measurements were taken directly from the electric motor with no load. This was done in order to minimize measurement errors. No load tests were conducted to measure potential power outputs and turbine RPM.
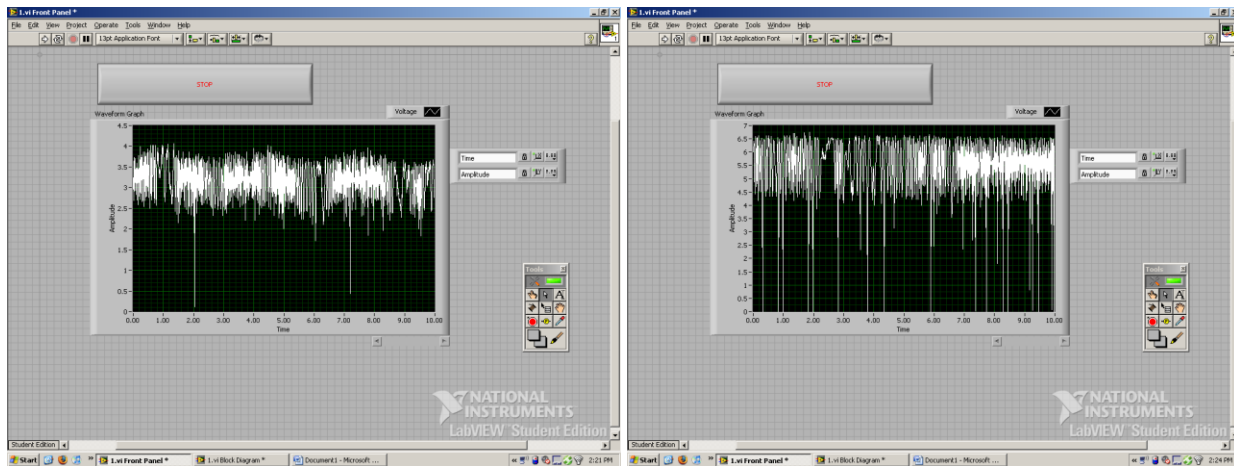
FIGURE 38-LABVIEW SCREENSHOTS

Using the Data Acquisition unit, the voltage output of the electric motor was measured at specific measured compressor output velocities. No-load tests were conducted with the turbine. Figure 38 shows two screenshots of the Labview setup during testing.

At three different compressed airspeeds, 1000 voltage measurements were taken over a period of ten seconds each. As you can see from Figure 39, the results contains noise, however, an average voltage was calculated at each of the three different compressed airspeeds to make calculations.
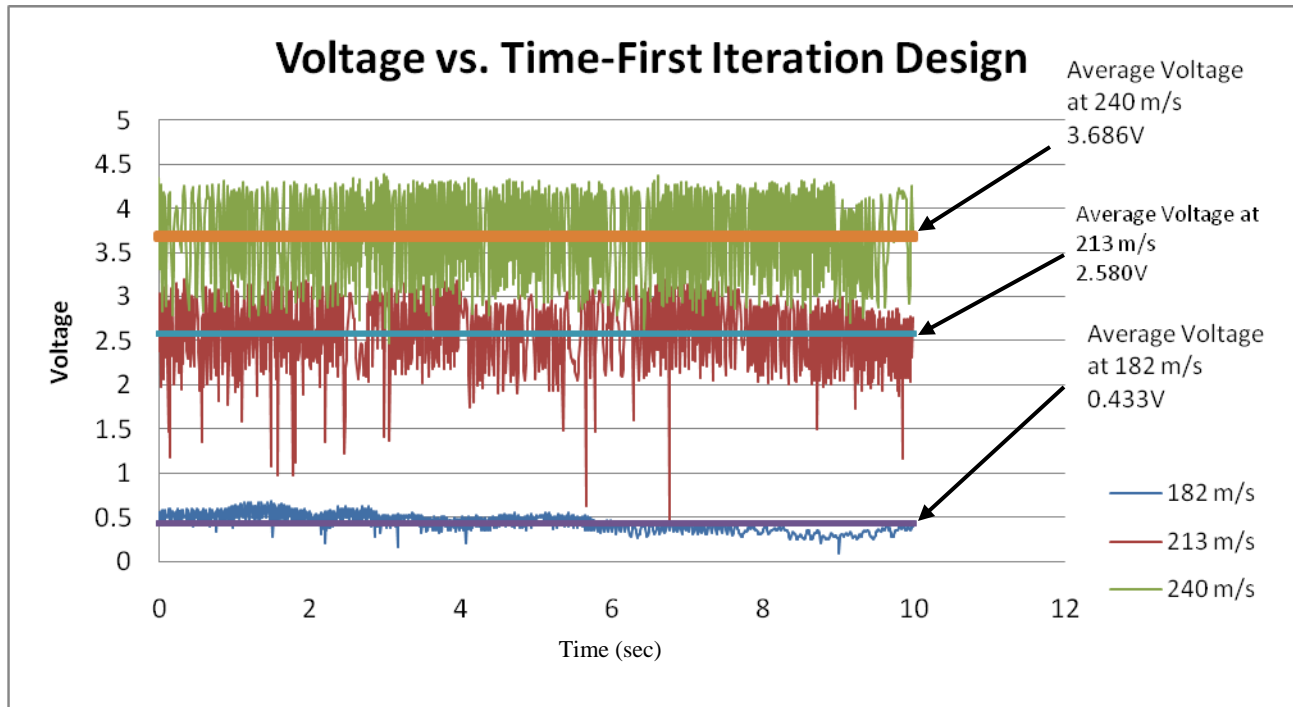
FIGURE 39- VOLTAGE FOR THREE DIFFERENT COMPRESSED AIRSPEEDS-FIRST ITERATION

Once an average voltage for each of the three different compressed airspeeds was established, power output was calculated for three varying loads of 10, 51, and 100 ohms. Given the voltage output (Vo), potential power output (P) could be measured for varying loads (R). Equation 18 was used to measure potential power output.

$$P = \frac{Vo}{R^2} \qquad (18)$$

Power was calculated for varying loads of 10, 51, and 100 ohms. Each data point represents the average of 1000 voltage measurements taken at each compressed air velocity. The maximum achievable power with the first iteration micro-turbine and a 10 ohm resistor is approximately 1.4 Watts. The results are plotted below in Figure 40.
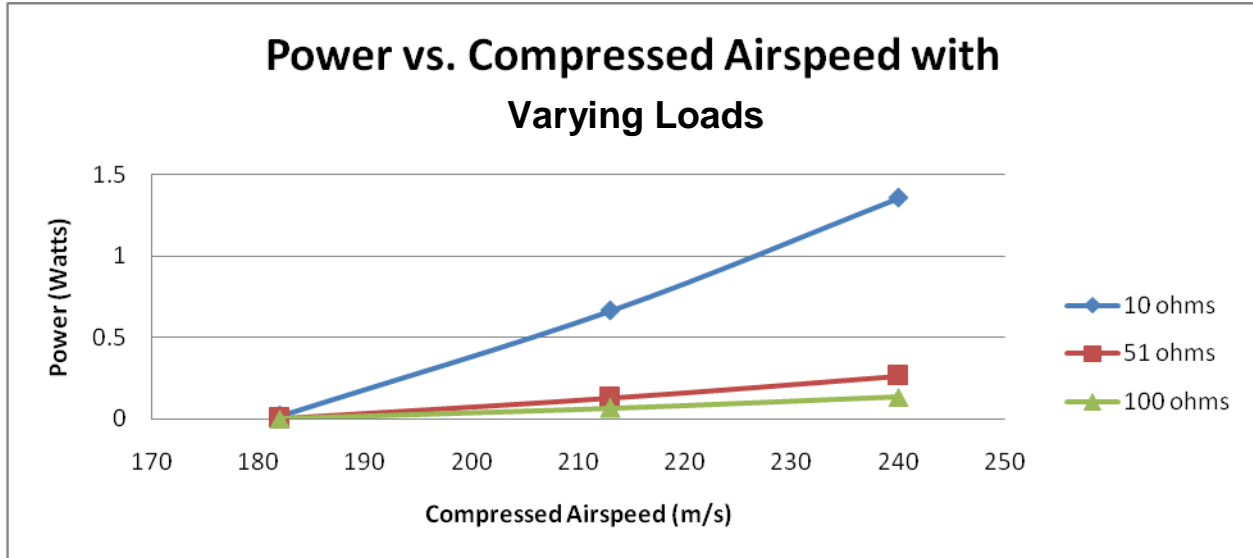
FIGURE 40-POWER FROM MICRO-TURBINE VS. COMPRESSED AIRSPEED

Also using the voltage output, turbine RPM could be measured using the electric motor's maximum voltage (Vm) output and the maximum RPM (Rm). Equation 19 was used to measure RPM .

$$RPM = \frac{Rm}{Vm}Vo \qquad (19)$$

It was assumed that the relationship between voltage output and RPM was linear. It was also assumed that at the maximum voltage output, the turbine would be spinning at the maximum RPM. The maximum RPM and voltage for the 9V motor was 25,000 and 9 respectively. The power equation above then becomes equation 20.

$$P_{max} = \frac{25000}{9}V_{compressed\,air} \qquad (20)$$

The maximum achievable RPM with the first iteration micro-turbine is approximately 10,000. The micro-turbine RPM was calculated at different compressed airspeeds using the average measured voltage. The results are plotted below in Figure 41.

FIGURE 41-RPM VS. COMPRESSED AIRSPEED

4.2 EXPERIEMNTAL TESTING OF SECOND ITERATION DESIGN

The results in this next section are for the second iteration turbine. The testing setup was the same as previously mentioned. The same motor was used. The compressed airspeed was measured and then the voltage across the motor was measured with no load.
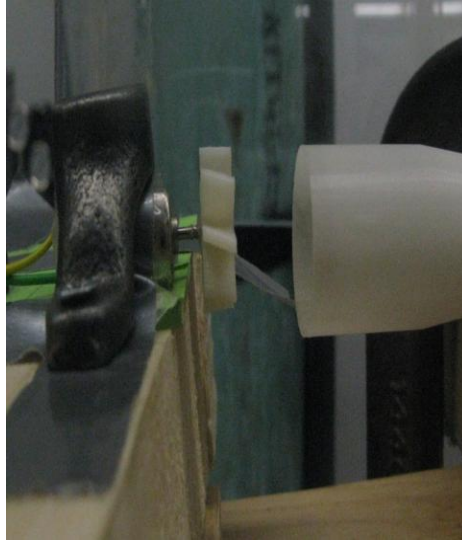
FIGURE 42-SECOND ITERATION TURBINE TEST SETUP

At three different compressed airspeeds, 1000 voltage measurements were taken over a

period of ten seconds each. As you can see from Figure 43, the results contained a lot of noise. An

average voltage was calculated at each compressed airspeed.

FIGURE 43- VOLTAGE VS. TIME FOR 0.25 INCH TURBINE

Once an average voltage for each compressed airspeed was established, power output was calculated for three loads of 10, 51, and 100 ohms. The results are plotted in Figure 44.
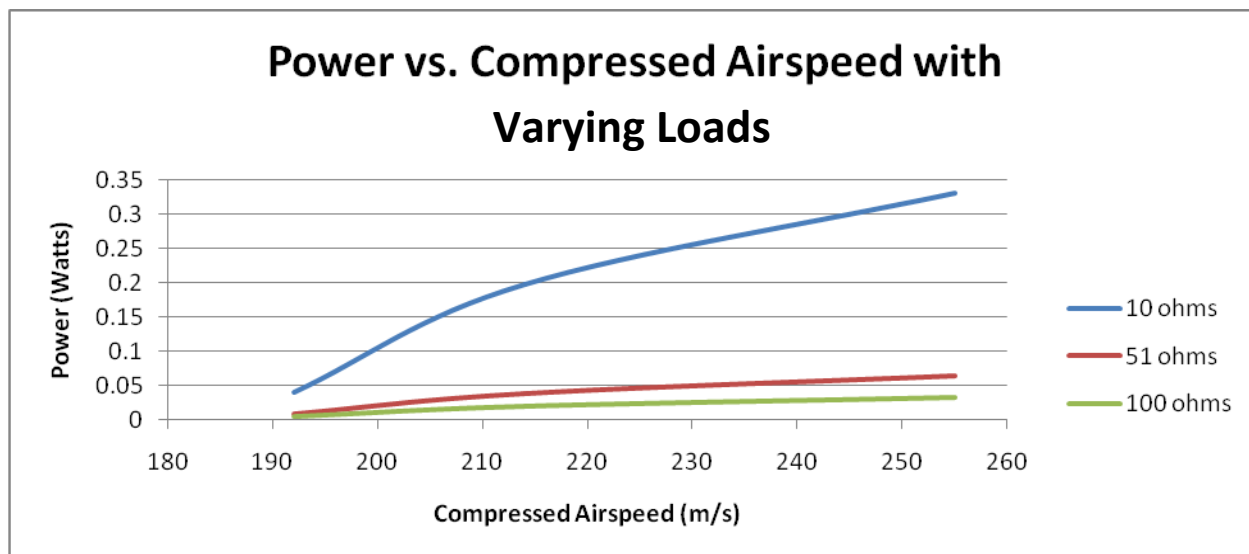
FIGURE 44-SECOND ITERATION-POWER VS. COMPRESSED AIRSPEED WITH HYPOTHETICAL LOADS

Each data point represents the average of 1000 voltage measurements taken at different compressed airspeed. Equation 14 was used to calculate power. The maximum achievable power with the second iteration micro-turbine and a 10 ohm resistor is approximately 0.35 Watts.

The micro-turbine RPM was also calculated at different compressed airspeed using the average measured voltage. The results are shown in Figure 45.
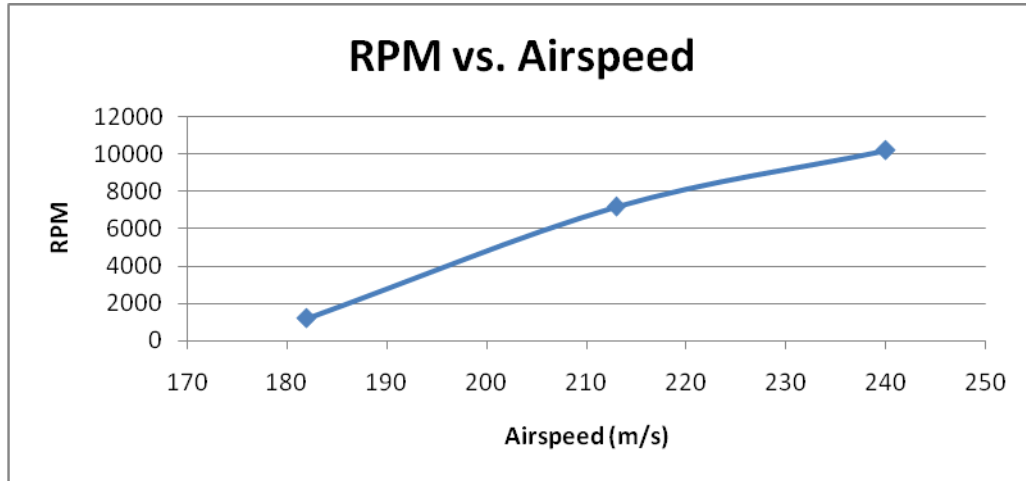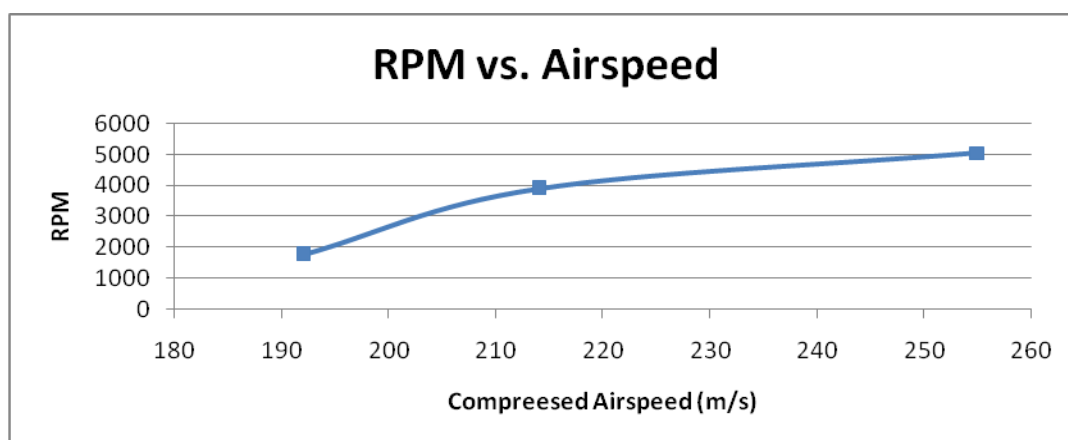

FIGURE 45-SECOND ITERATION-RPM VS. COMPRESSED AIRSPEED

Equation 15 was use to calculate the RPM. The maximum achievable RPM with the second iteration micro-turbine is approximately 5000.

4.3 EXPERIMENTAL TESTING OF THIRD ITERATION DESIGN

After testing the second iteration design, a third design was made in order to measure the effect of length on voltage output.

At three different compressed airspeeds, 1000 voltage measurements were taken over a span of ten seconds. As you can see from Figure 48-47 the results contain noise so an average voltage was calculated at different compressed airspeeds.
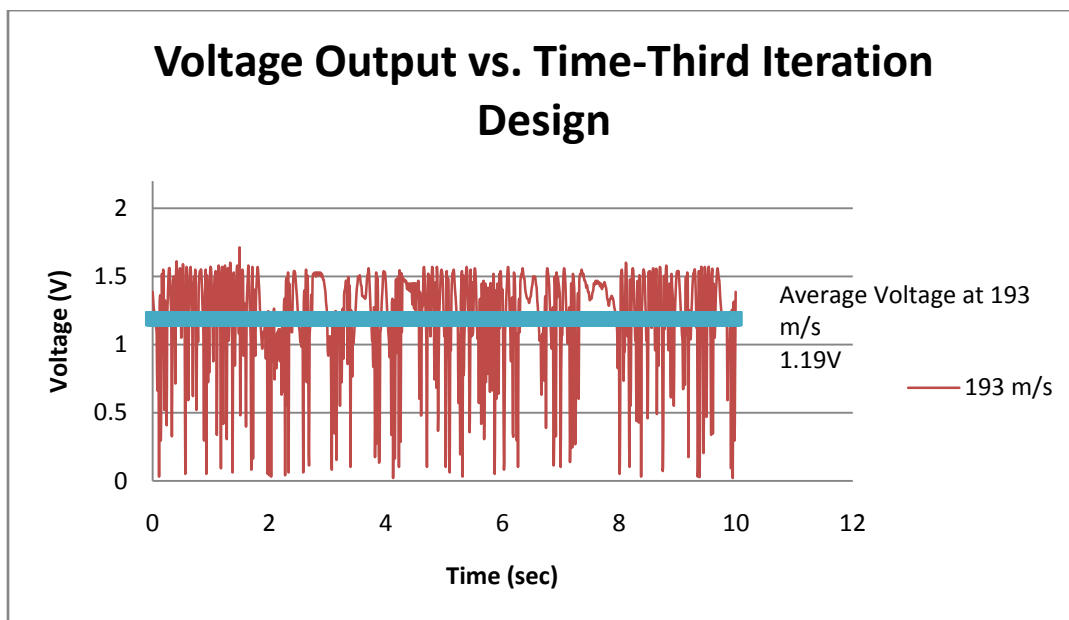
FIGURE 46-THIRD ITERATION- TIME VS. VOLTAGE OUTPUT AT 193M/S
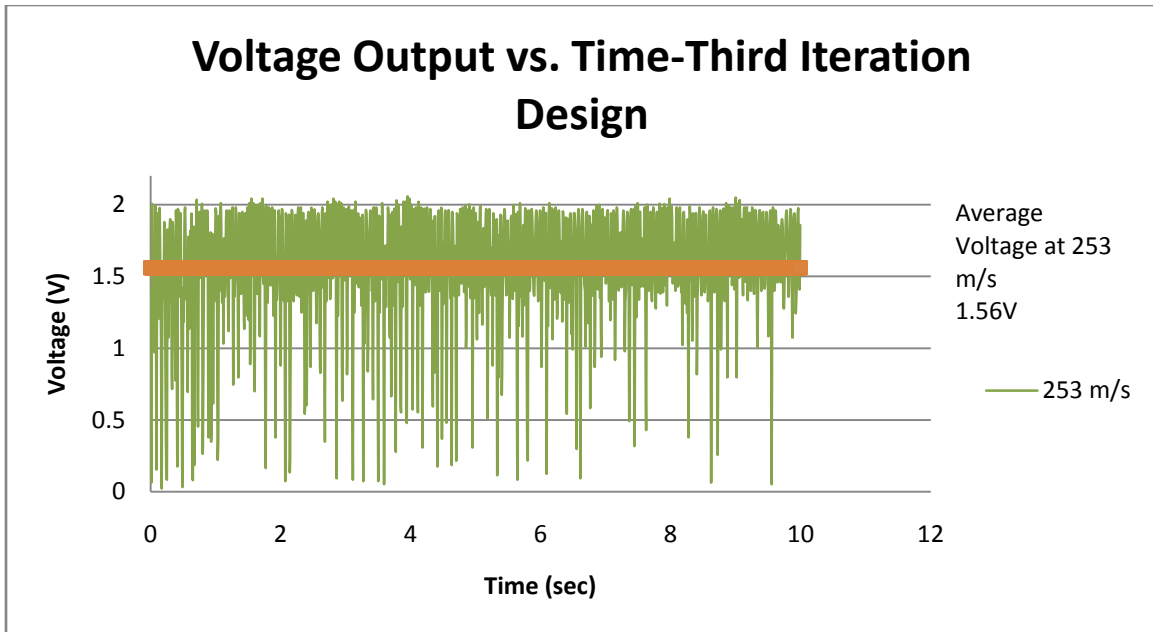
FIGURE 47-THIRD ITERATION- VOLTAGE OUTPUT VS. TIME- 253M/S
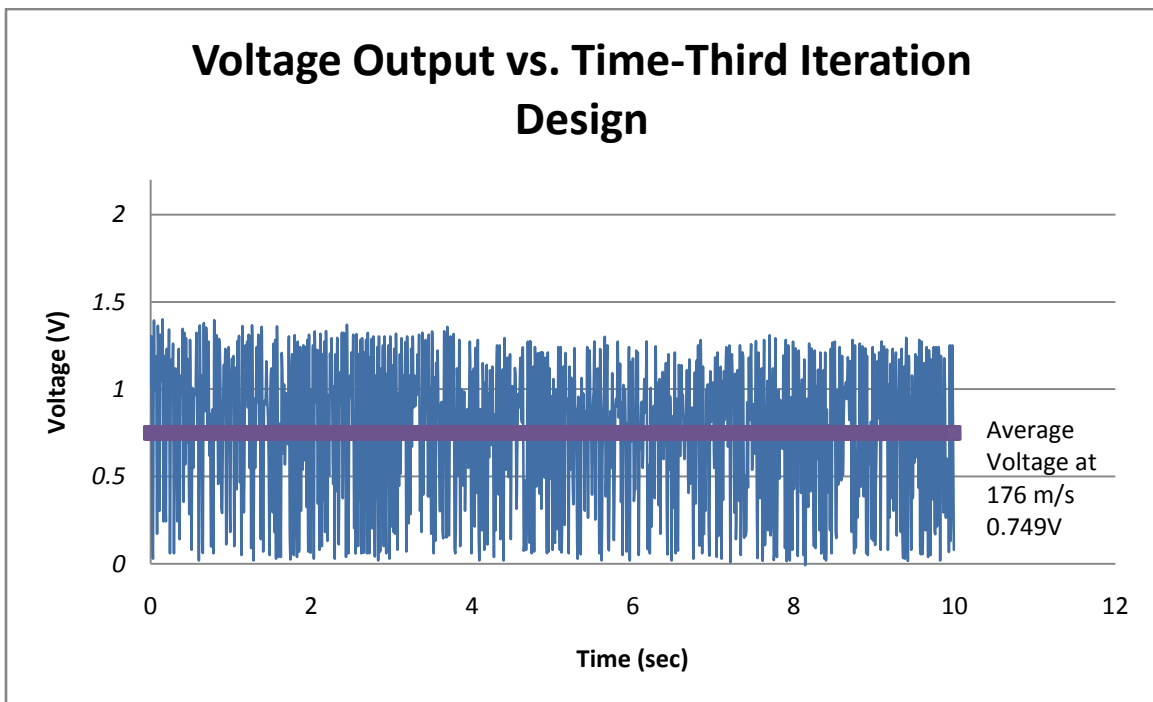
FIGURE 48- THIRD ITERATION- VOLTAGE OUPUT VS. TIME- 176M/S

Once an average voltage for the compressed airspeeds was calculated, the power output
was calculated for three hypothetical loads of 10, 51, and 100 ohms. The results are plotted below
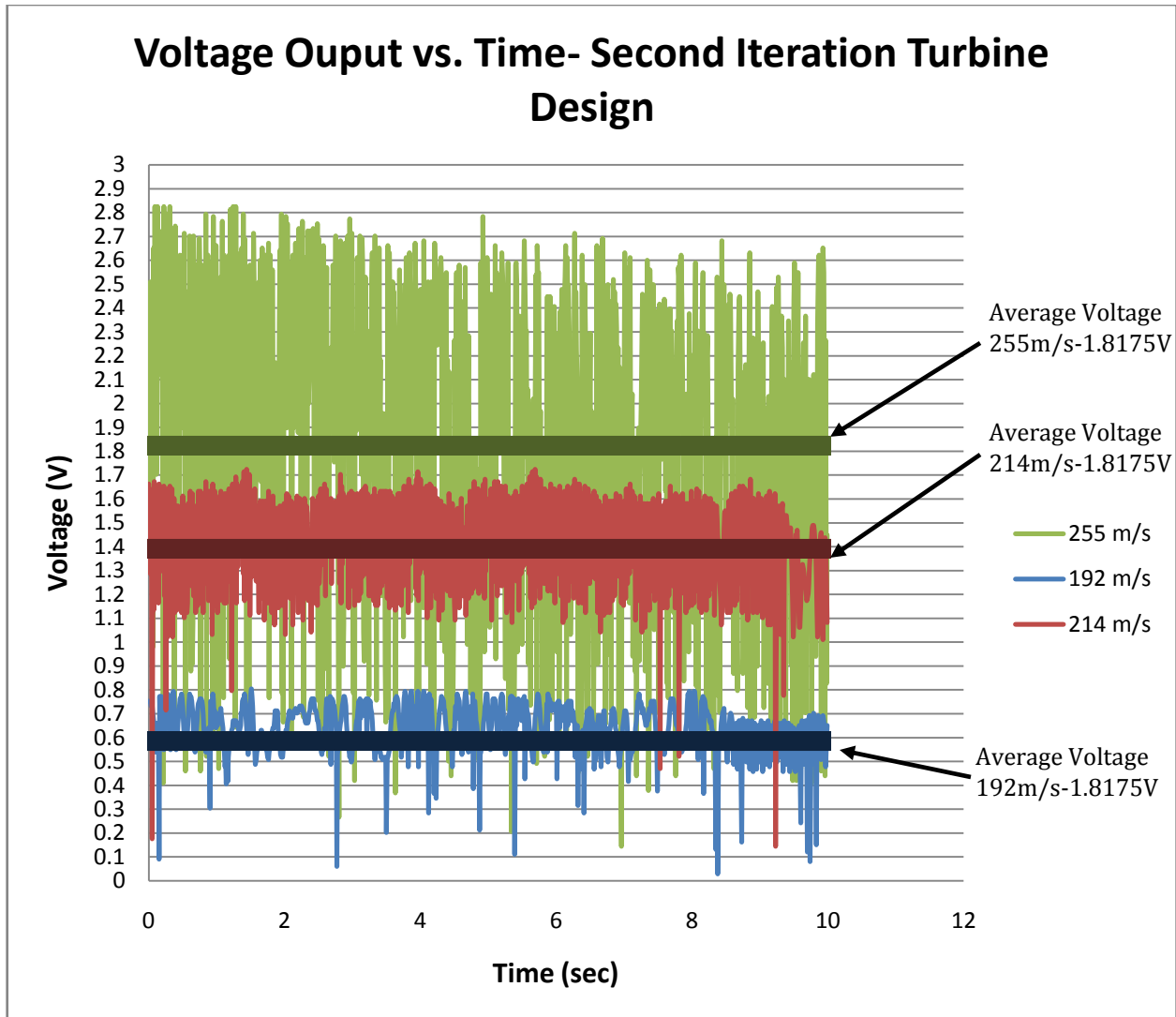in Figure 49.
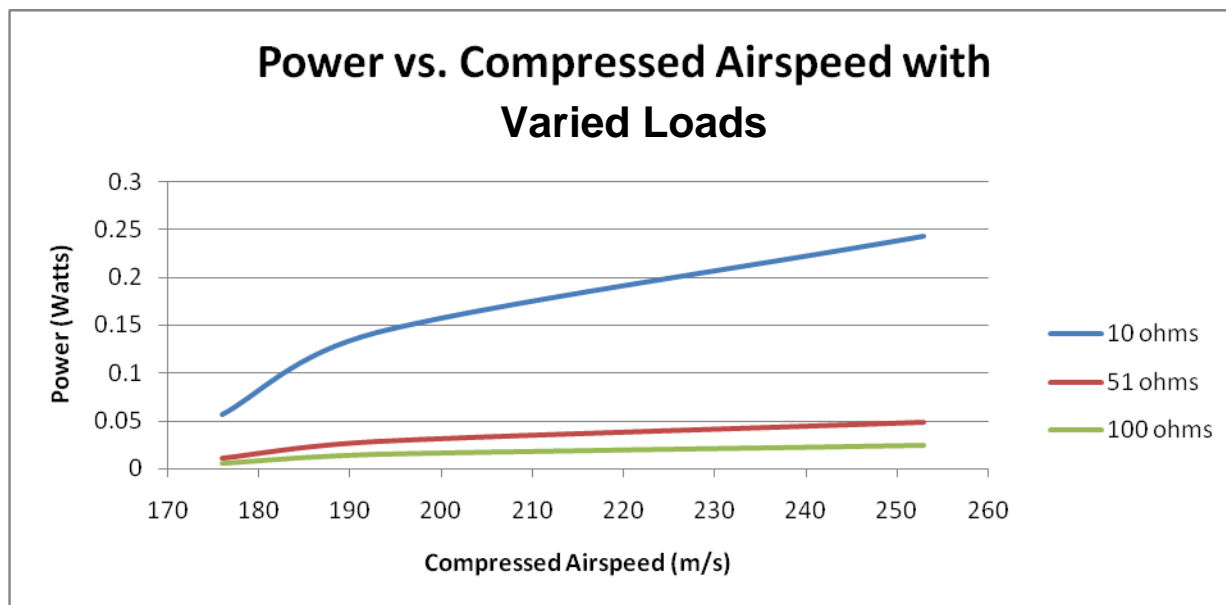
FIGURE 49-THIRD ITERATION-POWER VS. COMPRESSED AIRSPEED

Each data point represents the average of 1000 voltage measurements taken at different
compressed airspeeds. Equation 18 was used to calculate the power output. The maximum
achievable power with the third iteration micro-turbine and a 10 ohm resistor is approximately
0.25 Watts.

The micro-turbine RPM was also calculated at each compressed airspeed using the average
measured voltage. The results are plotted below in Figure 50.
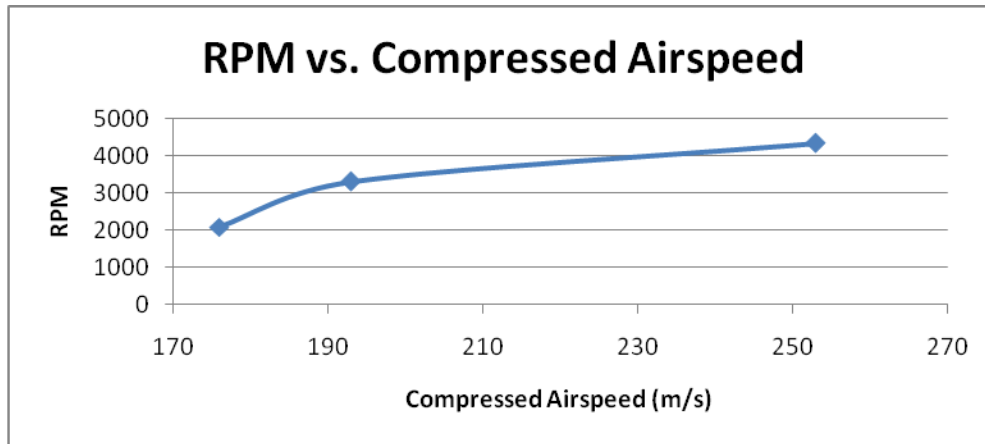
FIGURE 50-RPM VS. COMPRESSED AIRSPEED- THIRD ITERATION DESIGN

The equation used to calculate RPM was RPM = (25000/9)*V. The maximum achievable RPM with the third iteration micro-turbine is approximately 4300.

4.4 PACKAGING OF MICRO-TURBINE

As specified by Justin Urban of Pratt and Whitney, the micro-turbine package should be no larger than 1x1x3 inches. The packaging was originally going to be made of lexan material but was then changed to a small modified electrical box. This box holds the motor, wires, diodes and battery pack for the turbine. Figure 51and Figure 52 show the first micro-turbine and motor in the packaging.
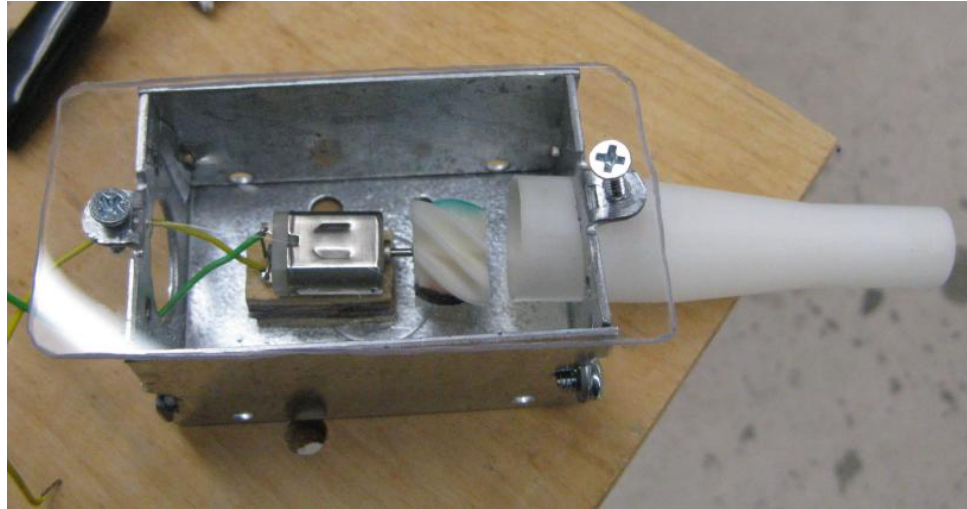
FIGURE 51-MICRO-TURBINE PACKAGING WITH NOZZLE
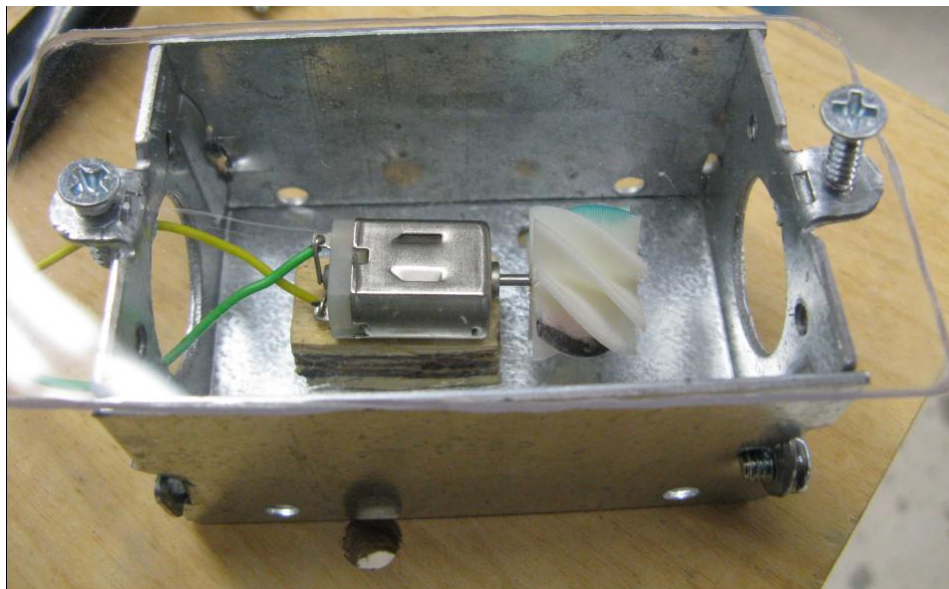
FIGURE 52- MICRO-TURBINE PACKAGING

5 STRESS ANALYSIS OF MICRO-TURBINES

Stress analysis was conducted on the micro-turbine due to air forces and centripetal forces. The following section outlines the micro-turbine stress calculations.

5.1 FIRST ITERATION DESIGN

For the following calculations, RPM=6000 and Power=.03 Watts. The mass of the turbine is .0045359 kg as calculated by Solidworks ©.

The stress due to the air forcing the turbine to move was calculated by using equation 21. Torque is the torque on the blades and f is the frequency (spin rate).

$$Torque = \frac{Power\_Output}{2\pi f} \tag{21}$$

The tangential force on the blades was calculated by using equation 22, where r is the radius of the micro-turbine.

$$F_{\text{tangential}} = \frac{Torque}{r_{turbine}} \tag{22}$$

For the first iteration turbine, the tangential force was calculated to be about .005N. Using SolidWorks ©, the stress can be modeled on the turbine design. Figure 53 shows the area of maximum stress is near the center, where the turbine is attached to the motor. The stress there is about 7016 N/m^2. This is not very much stress because the area where the maximum stress occurs is only 1.4251×10^{-4} m^2.
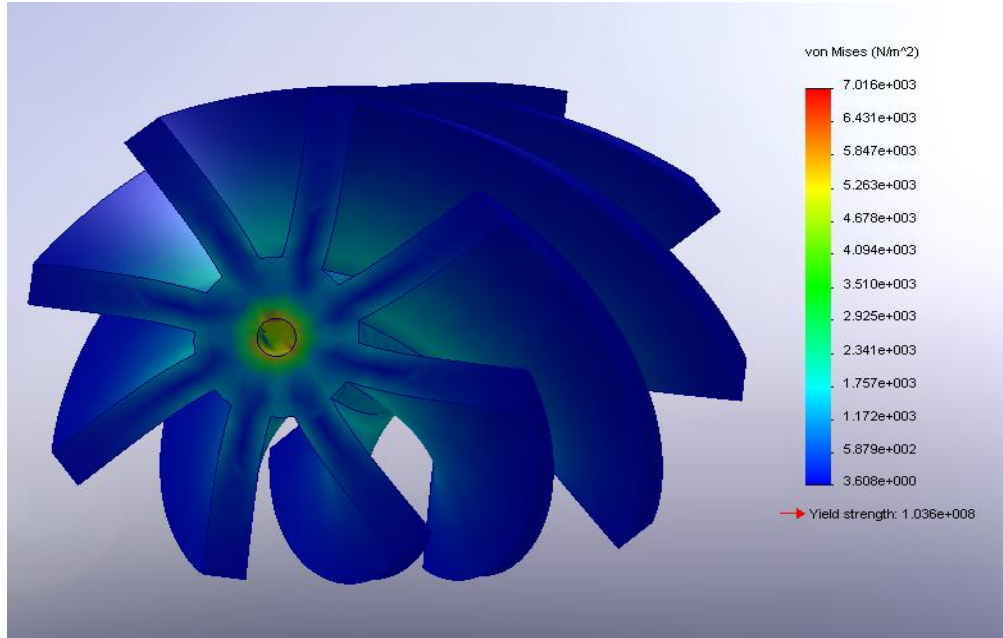
FIGURE 53-TANGENTIAL STRESS ON BLADES

To find the stress due to the rotation of the turbines equations 21 and 22 were used.

Equation 23 finds the centripetal acceleration of the turbine when it is spinning at 6000RPM.

$$a_{cent} = \omega^2 r \qquad (23)$$

The centripetal acceleration was found to be 1788.886 rad/sec. When multiplied by the

mass of the turbine, as shown in equation 24, the centripetal force was found to be 8.114N

$$F_{cent} = ma_{cent} \qquad (24)$$

Using CosmosWORKS ©, the centripetal forces were found on the turbine. Figure 55 shows

the stress due to the rotation of the turbine. The maximum stress is 314000 N/m^2 on the tips of the

turbine. Figure 54 shows a summary of the stress analysis results for the first micro-turbine.

Torque	$4.7746*10^{-5}$N*m
Tangential Force	0.005N
Centripetal Acceleration	1788.9 rad/sec^2
Centripetal Force	8.114N

FIGURE 54 -SUMMARY STRESS ANALYSIS TURBINE 1
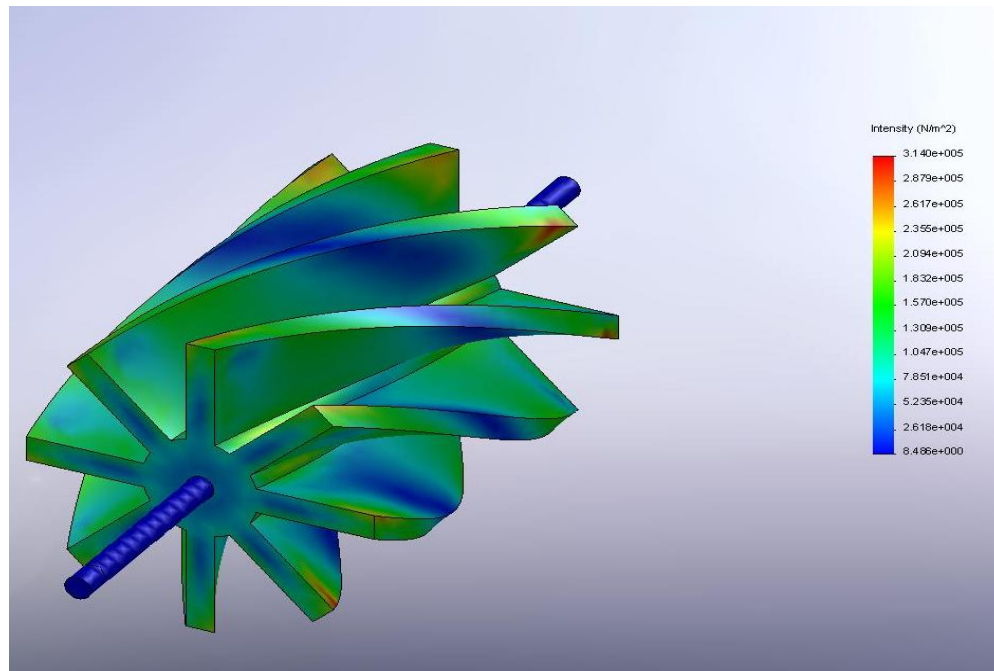
FIGURE 55-STRESS DUE TO ROTATION ON FIRST ITERATION TURBINE

5.2 SECOND ITERATION DESIGN

The stresses were found on the second iteration turbine in the same way as the first

iteration design. For this section of calculations, RPM was set to 6000 and power output was 0.2

Watts. The mass of the turbine is 0.00071867 kg as calculated by SolidWORKS ©. Figure 56

shows the results from using equations 21-24 on the second turbine iteration.

Torque	$3.183*10^{-5}$ N*m
Tangential Force	0.0033418 N
Centripetal Acceleration	3756.5 rad/sec^2
Centripetal Force	2.6996 N

FIGURE 56- SECOND ITERATION FORCES

After running the above number in SolidWORKS, the stress distribution is shown in Figure 57. The maximum stress is $2.707*10^4$ N/m^2. The turbine is only 0.25 inches long and converting to inches squared, the maximum amount of stress over the area is about 17.4644 N/in^2.
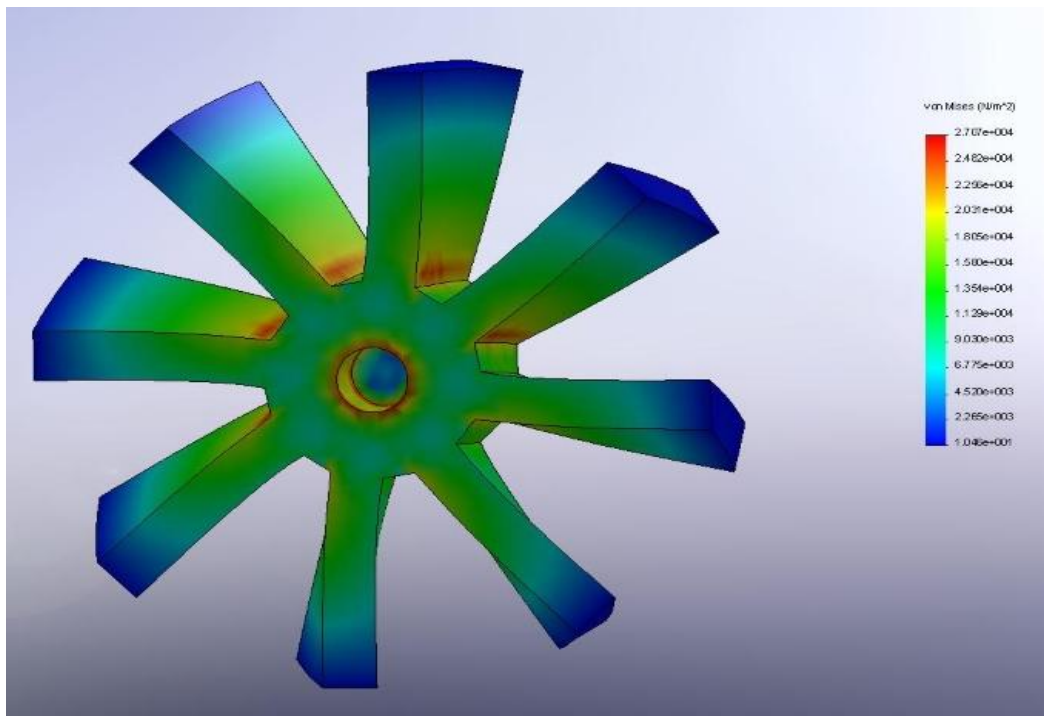
FIGURE 57-STRESS ON SECOND TURBINE DESIGN

5.3 THIRD ITERATION DESIGN

For this section of calculations, RPM was set to 6000 and power output was 0.2 Watts. The mass of the turbine is 0.0029619 kg as calculated by SolidWORKS ©. Using equations 21-24, information shown in Figure 58 was solved for.

Torque	$3.183*10^{-5}$N*m
Tangential Force	0.003255 N
Centripetal Acceleration	3864.56 rad/sec^2
Centripetal Force	11.446 N

FIGURE 58- STRESS ANALYSIS FOR THIRD ITERATION DESIGN

Figure 59 shows the stress on the turbine. The maximum stress is $7.290*10^4$. Due to the turbine being longer than the other two turbines, the stress distribution is spread out.
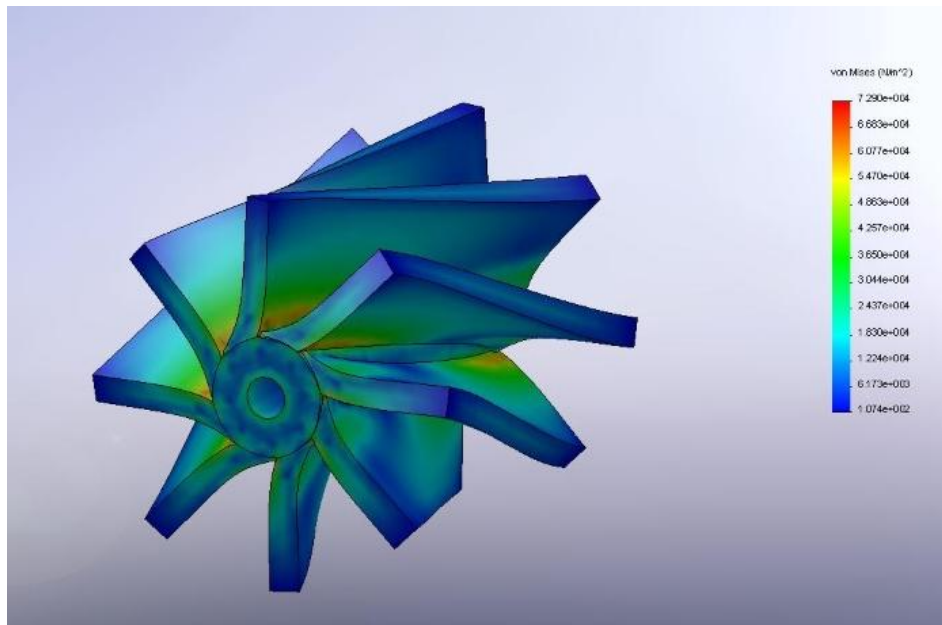
FIGURE 59-STRESS ON THIRD ITERATION TURBINE

6 CONCLUSIONS AND RECCOMMENDATIONS FOR FUTURE WORK

After testing all turbines, summary graphs and charts were made to compare the different designs. Options for future work are also discussed in this section.

6.1 SUMMARY OF RESULTS

The following section displays summary figures for RPM, voltage and power output for the three different turbines designs.

6.1.1 AVERAGE VOLTAGE

Voltage was measured across the motor for a period of 10 seconds. The average voltage was calculated by averaging the voltage across the 10 second time period. As shown in Figure 60, the highest voltage for high compressed airspeed is the first iteration turbine.
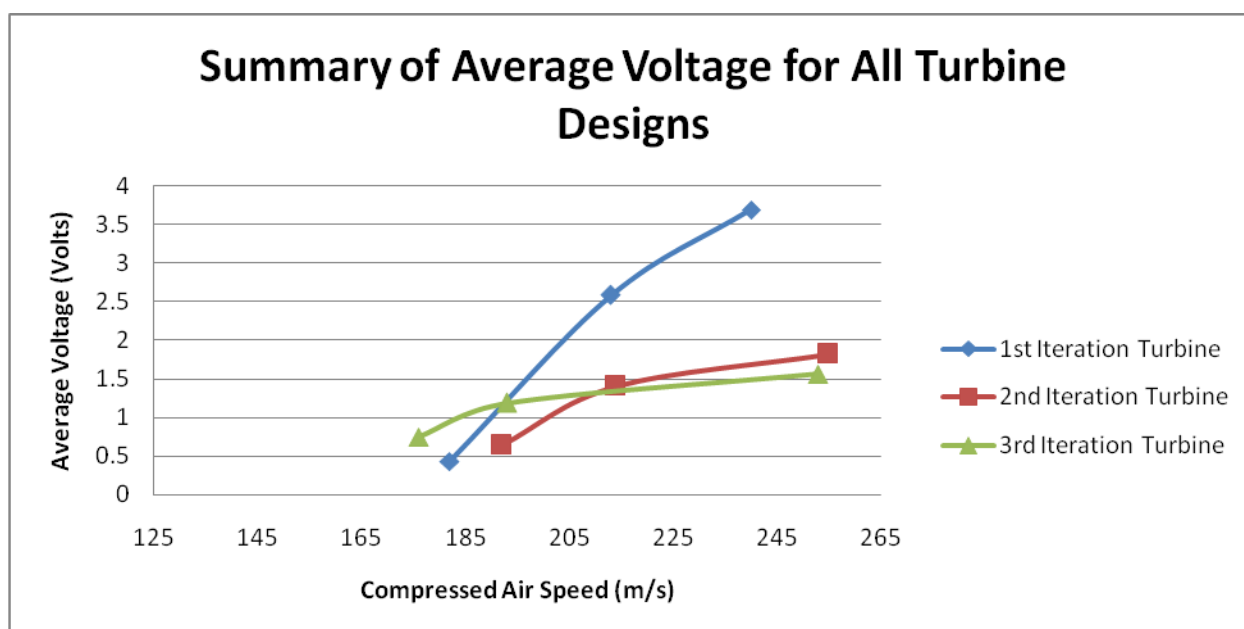
FIGURE 60- SUMMARY OF AVERAGE VOLTAGE-10 OHMS RESISTANCE

At lower speeds, the third iteration turbine has the highest voltage while the second iteration was lowest. The 3rd iteration turbine was the longest turbine designed while the second iteration was the shortest. This may indicate that the length of the turbine affects the voltage at speeds below ~200m/s.

6.1.2 RPM MEASUREMENTS

The micro-turbine RPM was calculated by comparing the measured voltage to the motor's maximum achievable voltage. At 9V, the motor is rated to spin at 25000 RPM. Assuming a linear relationship, the actual RPM can be calculated by multiplying the measured voltage by 25000/9. Figure 61 displays the calculated RPM for each of the three micro-turbines.
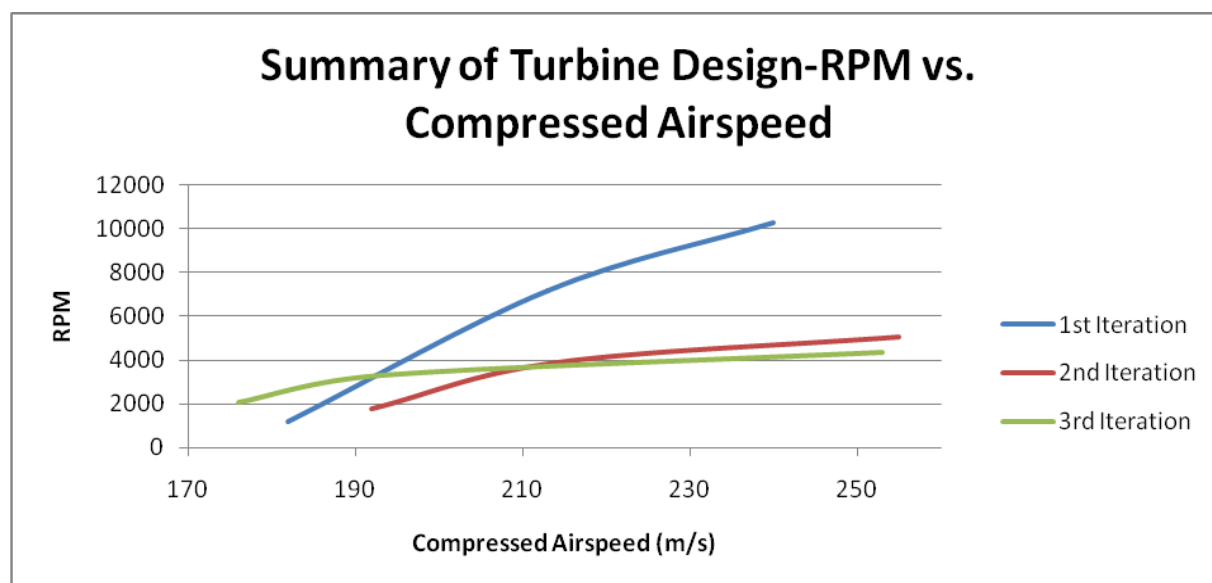
FIGURE 61-SUMMARY- RPM VS. COMPRESSED AIRSPEED-10 OHMS RESISTANCE

At lower velocities, all three turbines spin at approximately 2000 RPM. With increased velocities, however, the second and third iterations level out near 4000 RPM, whereas the first iteration continues to increase to over 10000 RPM. All maximum RPM's are measured at

compressed airspeeds slightly less than Mach 0.8, which is the maximum airspeed encountered in the secondary flow of the jet engine.

6.1.3 MICRO-TURBINE POWER OUTPUT
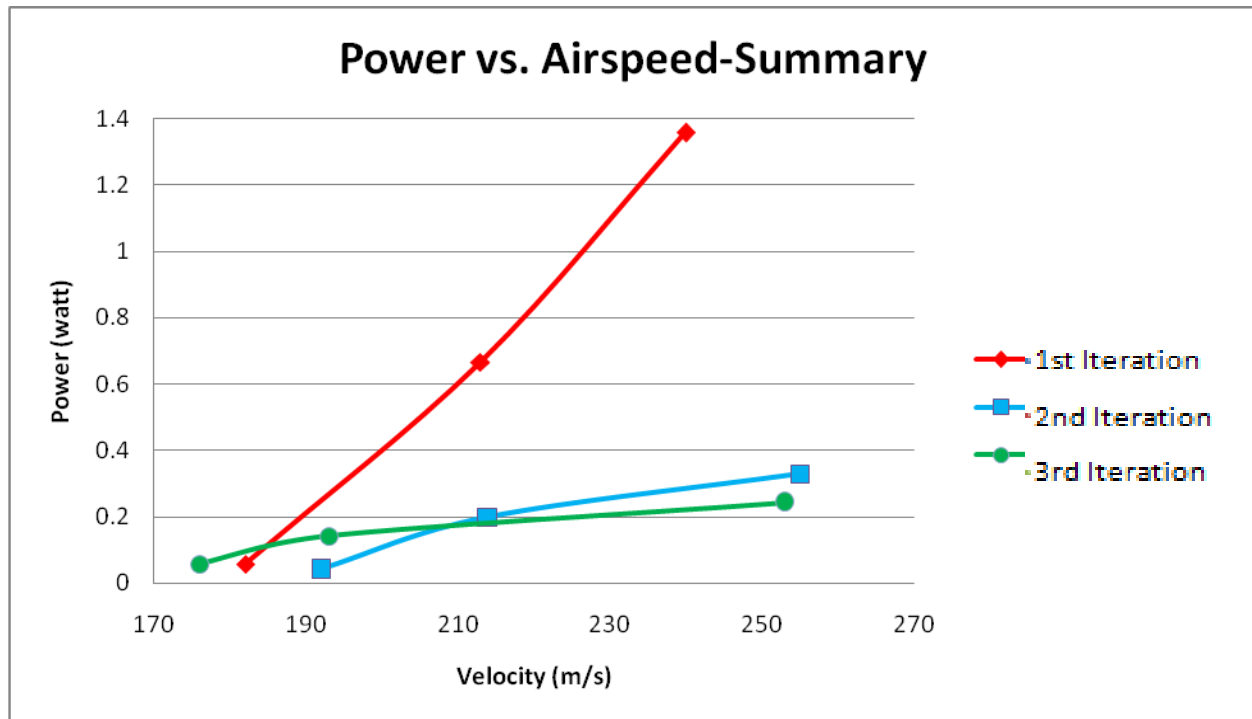
FIGURE 62- POWER VS. COMPRESSED AIRSPEED-SUMMARY--10 OHMS RESISTANCE

As shown in Figure 62, the first iteration turbine design generated the most power at most of the velocities tested. At the extreme low end of the velocities, the third iteration design produced the most power, while at the upper ranges it produced the least. Typical air velocities in the fan flow of a jet engine range from about 70 m/s to 270 m/s. In the upper half of these velocities, the first iteration would be best the best option for the most power. In the lower half the third iteration would be the best option for the most power.

6.2 FUTURE WORK

From the testing and design experience detailed in this report, conclusions and ideas for possible future work were made.

A main goal of any future project should be to increase power output of the micro-turbine. Possible methods to accomplish this include using modern airfoil shapes instead of flat flats for turbine blades and adding a fixed stator stage (pre-swirler) upstream of rotating turbine to direct inlet flow into turbine stage. Use different motors as generators might also change the power output. s

The material selection for the micro-turbine can be changed to meet Pratt and Whitney's needs. The rapid prototyping ABS plastic provides a lightweight and cheap way to make the small turbines but the smaller the turbine, the more likely there will be errors in the printing/manufacturing process. ABS plastic is also recyclable. The ABS plastic used with the WPI rapid prototyping machine does not display a melting point due to the amorphous nature of the material. Appendix II has the material properties of the ABS plastic used in the WPI rapid prototype. Even though the ABS plastic used may not melt, it may deform at high temperatures. The temperature in the fan flow of the gas turbine engine is 130°F. If this type of energy scavenging were to expand to different, hotter sections of the engine, other materials, such as stainless steel as used by the Micro and Precision Engineering Research Group, would need to be used. Stainless steel has a melting point of over 1380°F and is still relatively inexpensive and can be recycled. It does however, have a higher density than the ABS plastic which increase the weight of the micro-turbine and decrease the rotational speed. Composites may also be another option although they are more expensive and harder to manufacture.

One thing that may help future work is to have an air source that puts out a constant stream of air. The speed of the compressed air source used would sometimes fluctuate without notice. This would then change the voltage output which would then change the possible power output. Finding a completely steady air source would alleviate this problem.

It may be beneficial to combine forms of energy scavenging in order to meet the required power for the sensors. By combining types of energy scavenging, such as thermal and wind, it may be possible to get more power to battery packs and sensors.

REFERENCES

Bradway, Daniel, Daniel Bryant, Gregory Bukowski and Corina Scanio. Thermal Energy

    Scavenging To Power Aircraft Engine Test Sensors, MQP Report, Worcester Polytechnic

    Institute, 2008.

DeAnna, R. G. (2000). Wireless Telemetry for Gas Turbine Applications. NASA.

    gltrs.grc.nasa.gov/reports/2000/TM-2000-209815.pdf .

Environmental Hazard of Batteries. Environmental Health and Safety Online. 2006.

    http://www.ehso.com/ehshome/batteries.php#Hazards

Fox, Robert W., McDonald, Alan, T. Introduction to Fluid Mechanics (2004). New Jersey: John

    Wiley and Sons.

Micro and Precision Engineering Research Group. *Micro-turbine for electric power generation.*

    Katholieke Universiteit Leuven. 2005.

    <http://www.mech.kuleuven.be/micro/topics/turbine/>

Moody Diagram. EngineeringToolbox.com.

    <http://www.engineeringtoolbox.com/docs/documents/618/moody-diagram-2.png.>

    Accessed 20 March 2009.

Nice, Karim. "How Turbochargers Work." 04 December 2000. HowStuffWorks.com.

    <http://auto.howstuffworks.com/turbo.htm> Accessed 12 October 2008.

Roundy, S. Wright, P.K. et al. (2004). ENERGY SCAVENGING FOR WIRELESS SENSOR

    NETWORKS. Boston: Klumer Academic Publishers

Roundy, Shad, Dan Steingart, Luc Frechette, Paul Wright, and Jan Rabaey. Power Sources for

Wireless Sensor Networks. 2004. Berlin Germany.

http://www.springerlink.com/content/b0utgm8ahnphll3l/fulltext.pdf

Paradiso, Joseph and Thad Starner. Energy Scavenging for Mobile and Wireless Electronics. *IEEE*

CS and IEEE ComSoc issue 1536-1268/05, 2005.

http://ieeexplore.ieee.org/stamp/stamp.jsp?arnumber=01401839.

Thomas, James, Muhammad A. Qidwai , and James C. Kellogg. Energy Scavenging For Small-

Scale Unmanned Systems. Journal of Power Sources 159 (2006) 1494–1509. 2005

http://www.sciencedirect.com/science?_ob=MImg&_imagekey=B6TH1-4JBGJ45-6-

26&_cdi=5269&_user=74021&_orig=search&_coverDate=09%2F22%2F2006&_sk=99

8409997&view=c&wchp=dGLbVzb-

zSkzS&md5=6c9042941675c9e5d74fc1338c56d372&ie=/sdarticle.pdf

Drawings of the three micro-turbines

0.75

0.26

8 arms
Evenly spaced

<MOD-DIAM>.09

Helix:
7.76 in pitch
0.0321 revolutions

.25

3   2   1

Ø.09

Ø0.26

.06

A

A

8 arms
Evenly spaced

.50

SECTION A-A

12.00°

1.00

.75

UNLESS OTHERWISE SPECIFIED:	TITLE:		
DIMENSIONS ARE IN INCHES	Turbine Iteration 3		
	Worcester Polytechnic Institute		
COMMENTS:			
	SIZE A	DWG. NO. 1	REV
	SCALE: 2:1	SHEET 1 OF 1	
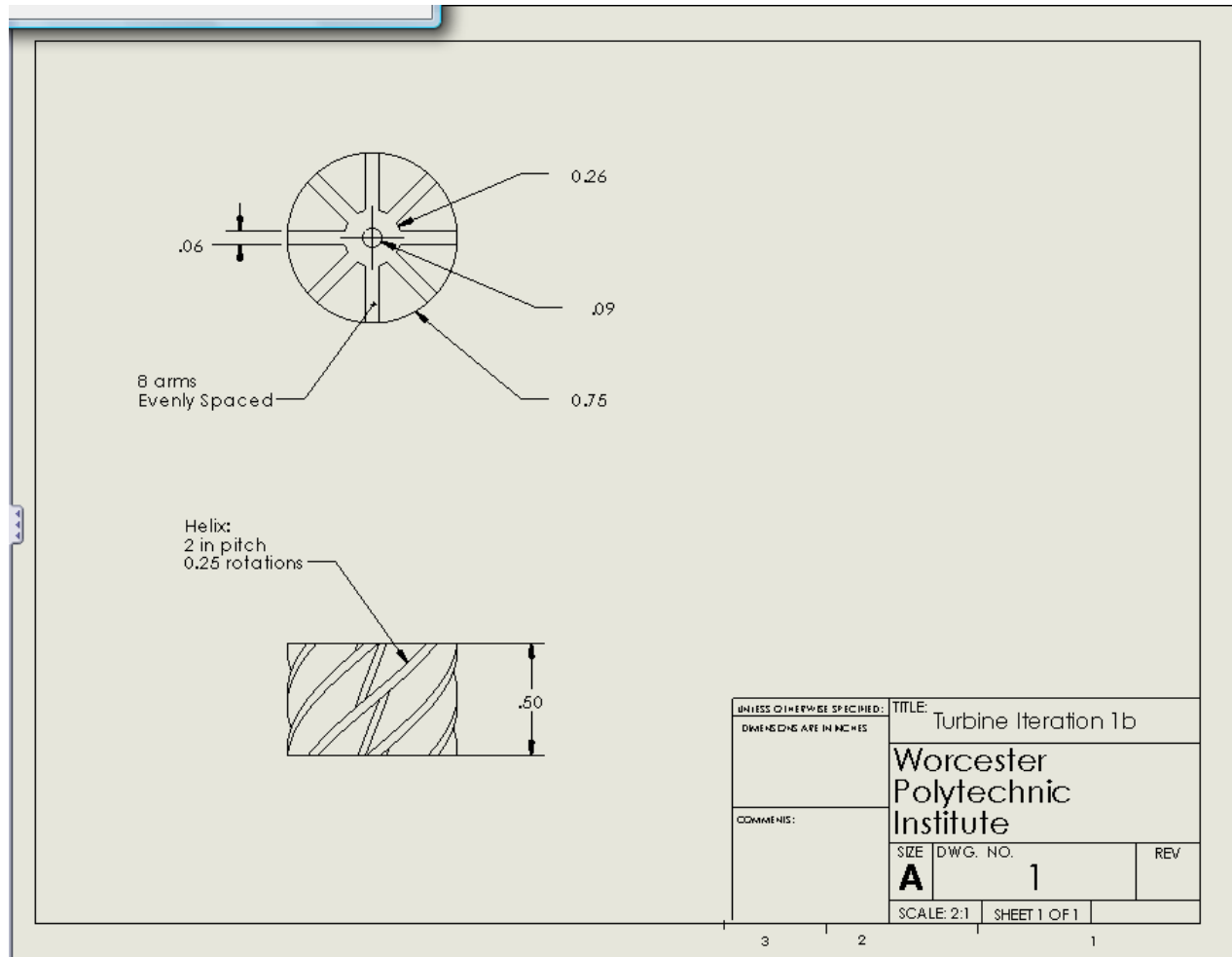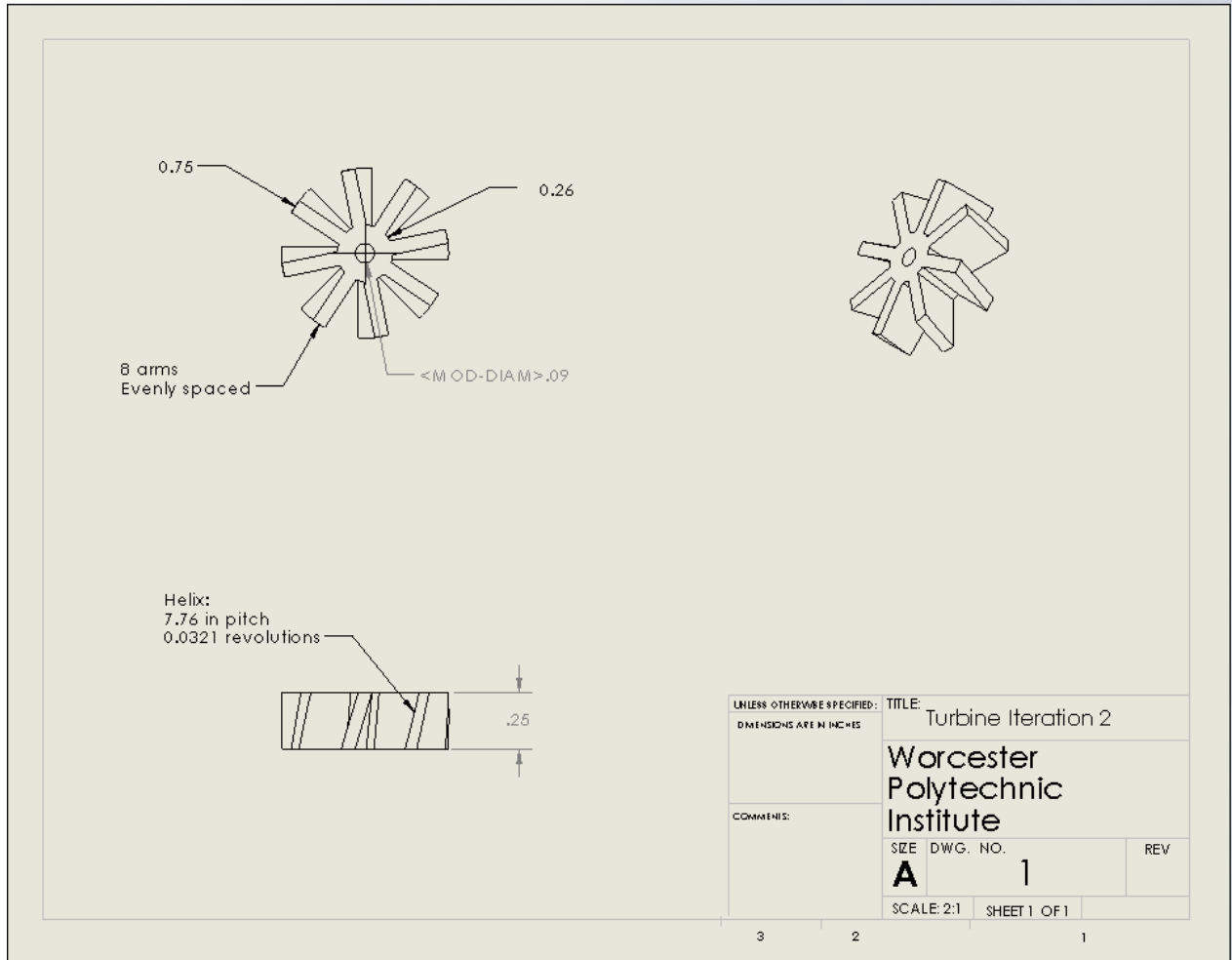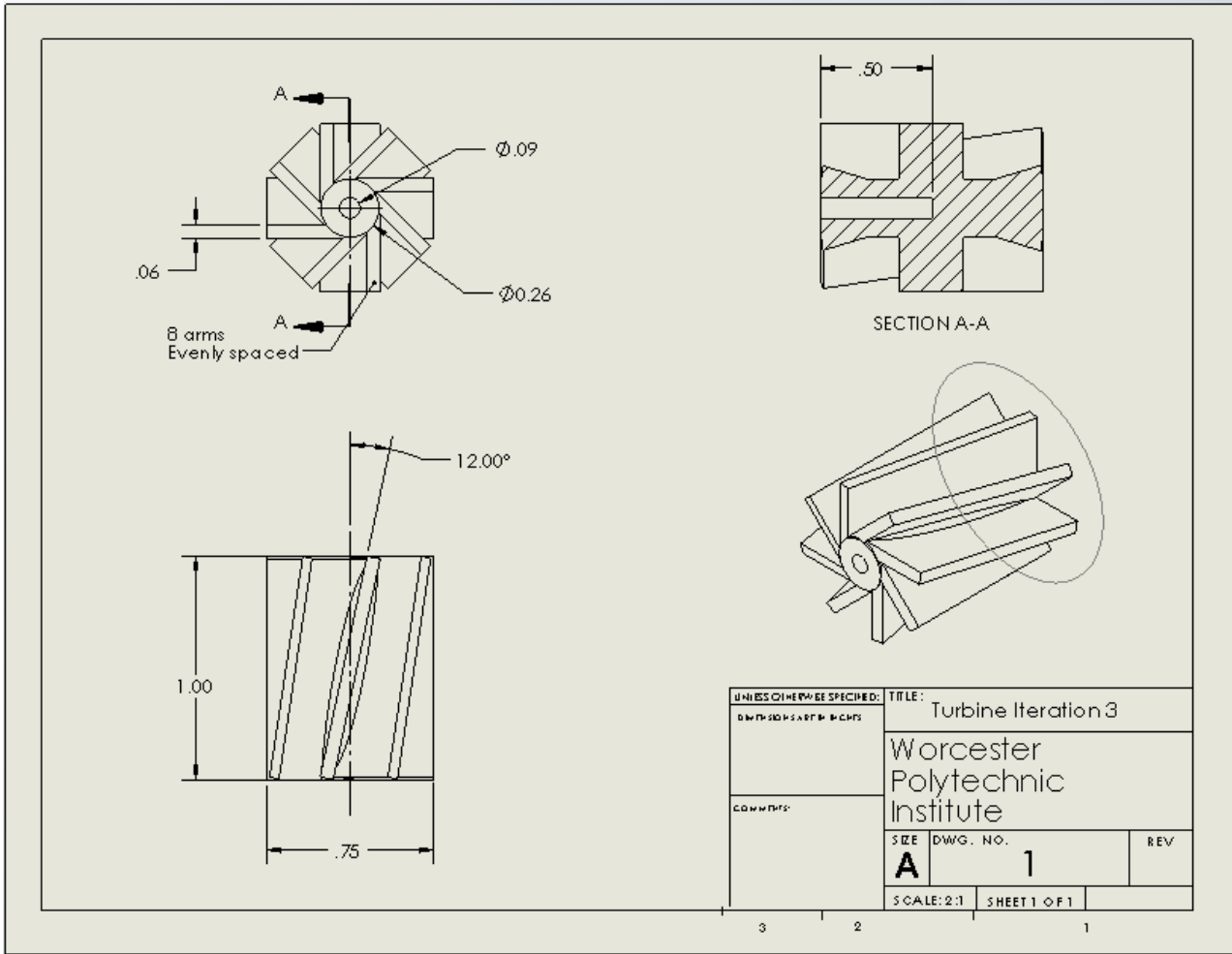
APPENDIX II- RAPID PROTOTYPING ABS PLASTIC MATERIAL PROPERTIES

http://www.aqm.it/_modules/download/download/Specifiche_ABS_rev2.pdf ; Accessed April 2, 2009

STRATASYS®

ABS
FDM Material Properties

A true industrial thermoplastic, ABS is widely used throughout industry. When combined with Dimension and the Fused Deposition Modeling process from Stratasys, this material is ideal for 3D printing of models in the engineering office.

MECHANICAL PROPERTIES[1]

	Test Method	Imperial	Metric
Tensile Strength, Type 1, 0.125	ASTM D638	3,200 psi	22 MPa
Tensile Modulus, Type 1, 0.125	ASTM D638	236,000 psi	1,627 MPa
Tensile Elongation, Type 1, 0.125	ASTM D638	6 %	6 %
Flexural Strength	ASTM D790	6,000 psi	41 MPa
Flexural Modulus	ASTM D790	266,000 psi	1,834 MPa
IZOD Impact, un-notched	ASTM D256	4 ft-lb/in	
IZOD Impact, notched	ASTM D256	2 ft-lb/in	

THERMAL PROPERTIES

	Test Method	Imperial	Metric
Heat Deflection (HDT)	ASTM D648	205 °F	96 °C
Glass Transition (Tg)	DMA (SSYS)	219 °F	104 °C
Melt Point		Not Applicable[2]	Not Applicable[2]

OTHER

Specific Gravity	1.05
Vertical Burning Test	HB, UL94
Coefficient of Thermal Expansion	5.60E-05 in/in/F
Rockwell Hardness	R105
Dielectric S (kV/mm)	32
Dielectric C (60Hz)	2.4

APPEARANCE

Standard colors include white, blue, green, yellow, black, red, and steel gray

Custom colors available

Stratasys, Inc.
14950 Martin Drive
Eden Prairie, MN USA 55344
Ph: 952.937.3000
Fax: 952.937.0070
www.dimensionprinting.com

SYSTEM AVAILABILITY

Dimension
Dimension BST
Dimension SST

The information presented are typical values intended for reference and comparison purposes only. They should not be used for design specifications or quality control purposes. End-use material performance can be impacted (+/-) by, but not limited to, part design, end-use conditions, test conditions, etc. Actual values will vary with build conditions.

Product specifications are subject to change without notice.

---

[1] Build orientation is on side edge
[2] Due to amorphous nature, material does not display a melting point

ABS_prop_050116 Mod.doc   Current as of 31 March 2005

STRATASYS®	**P400 ABS**
Material Safety Data Sheet	9/14/04

1. CHEMICAL PRODUCT & COMPANY IDENTIFICATION

Product Name	P400 ABS
Chemical Family	Styrene Terpolymer
General Use	Filament for Stratasys® Inc. FDM™ modeler
Manufacturer and Address	Stratasys Inc. 14950 Martin Drive Minneapolis, MN 55344-2020 USA
Emergency Telephone Number	+1 952-937-3000

2. COMPOSITION, INGREDIENT INFORMATION

COMPONENT	CAS #	%	OSHA/PEL	ACGIH/TLV
Acrylonitrile/butadiene/styrene resin	009003-56-9	90-100	N/E	N/E
May contain the following:				
Mineral Oil	008042-47-5	0-2	N/E	N/E
Tallow	067701-27-3	0-2	N/E	N/E
Wax	000110-30-5	0-2	N/E	N/E

N/E = not established. P400 (ABS) is not considered hazardous under the criteria of the Federal OSHA Hazard Communication Standard 29 CFR § 1910.1200

3. HAZARDS IDENTIFICATION

Emergency Overview	No significant immediate hazards for emergency response are known
HMIS Ratings	Health: 0 Flammability: 1 Reactivity: 0
Inhalation	Dust or vapors may be irritating to the respiratory tract and cause coughing or sneezing
Eye Contact	Dust or vapors that contact the eye may be irritating or cause corneal injury due to mechanical action
Skin Contact	Molten material will produce thermal burns
Ingestion	Very low toxicity if swallowed. Harmful effects not anticipated from swallowing small amounts.
Chronic	No relevant information found
Carcinogenicity	No relevant information found
Threshold Limit Value	No established value. Product is inert.

STRATASYS®	P400 ABS
Material Safety Data Sheet	9/14/04

4. EMERGENCY AND FIRST AID MEASURES

Inhalation	Move person to fresh air if effects occur. Consult a physician.
Skin Contact	If molten material comes in contact with skin, do not apply ice. Cool skin under ice water or running water. DO NOT attempt to remove the material from skin. Removal could result in severe tissue damage.
Skin Absorption	Skin absorption is unlikely due to physical properties
Eye Contact	Flush eyes with plenty of water. Remove contact lenses after the first 1-2 minutes then continue flushing for several minutes. Only mechanical effects expected.
Ingestion	No emergency medical treatment necessary

5. FIRE-FIGHTING MEASURES & EXPLOSION HAZARD DATA

Flash Point	None
Method Used	Not applicable
Flammability Limits: LFL, UFL	Not applicable
Autoignition Temperature	Not applicable
Extinguishing Media	Water, fog, foam, alcohol resistant foam, CO2, dry chemical
Special Fire-Fighting Procedures	Wear a positive pressure self-contained breathing apparatus (SCBA) and fire fighting clothing and helmet
Unusual Fire and Explosion Hazards	Dense smoke emitted when burned without sufficient oxygen
Hazardous Decomposition Products	During a fire, smoke may contain the original material in addition to combustion products of varying composition products, which may be toxic and/or irritating. Combustion products may include and are not limited to carbon monoxide, carbon dioxide, and nitrogen oxides. Combustion products may include trace amounts of styrene and hydrogen cyanide.
Fire Fighting Instructions	Keep people away from fire. Isolate fire area and deny unnecessary entry. If material is molten, do not apply direct water stream. Use fine water, spray, or foam. Soak thoroughly with water to cool and prevent re-ignition. Cool surroundings with water to localize fire zone. Hand held dry chemical or carbon dioxide extinguishers may be used for small fires.

STRATASYS®	**P400 ABS**
Material Safety Data Sheet	9/14/04

6. ACCIDENTAL RELEASE MEASURES

General	Protect people and the environment by keeping filament in appropriate locations
Specific	Sweep "inert" filament and dispose of properly. Avoid the generation of dust in the area.

7. HANDLING & STORAGE

Handling	Keep material dry and avoid temperatures over 70°C Those handling molten resin during fabrication should be protected from possible contact.
Storage	Store in a cool, well-ventilated area. Keep container tightly closed.

8. EXPOSURE CONTROLS & PERSONAL PROTECTION

Although some of the additives used in this product may have exposure guidelines, these additives are encapsulated in the product and no exposure would be expected under normal handling conditions.

Ventilation	Provide local exhaust ventilation where heat can cause polymer breakdown, e.g. extrusion, molding and where there is a need to draw dusts and fumes from worker breathing zones.
Respiratory	For conditions where exposure to dust and fumes is apparent, an NIOSH approved respirator for dust mists and fumes appropriate to the airborne concentration may be worn. Where vapors are generated, an NIOSH approved organic respirator suitable to the airborne concentrations is recommended.
Eye Protection	Safety glasses with side shields are recommended for any type of handling. Dust-tight goggles are recommended for dusty operations of areas where vapors accumulate.
Skin	No precautions other than clean body-covering clothing should be used. Use gloves for insulation for thermal protection, when needed.

![STRATASYS logo] **STRATASYS°**	**P400 ABS**
Material Safety Data Sheet	9/14/04

9. PHYSICAL & CHEMICAL PROPERTIES

Appearance	Milky off-white solid
Odor	Odorless
Vapor Pressure	Not applicable
Vapor Density	Not applicable
Melting Point	Not applicable
Boiling Point	Not applicable
Specific Gravity	1.05
Volatile By Volume (Water)	Not applicable
Solubility In Water	Nil
pH	Not applicable

10. STABILITY & REACTIVITY

Stability	Stable
Conditions to Avoid	Temperatures over 300° C (572° F) releases combustible gases
Hazardous Polymerization	Will not occur
Incompatibility	Oxidizing materials
Hazardous Thermal Decomposition Products	Decomposition products depend upon temperature, air supply, and the presence of other materials. At temperatures exceeding melt temperatures, polymer fragments can be released. Fumes can be irritating.

11. TOXICOLOGICAL DATA

Acute Oral	No data available. Not expected to be harmful.
Acute Dermal	No data available. Not expected to be harmful.
Acute Inhalation	No data available. Not expected to be harmful.
Skin Irritation	No data available. Not expected to be harmful.
Eye Irritation	No data available. Not expected to be harmful.
Genotoxicity	No data available. Not expected to be harmful.

STRATASYS®	P400 ABS
Material Safety Data Sheet	9/14/04

12. ECOLOGICAL INFORMATION

Movement and Partitioning	No bioconcentration is expected because of the relatively high molecular weight (MW >1000). In the terrestrial environment, material is expected to remain in the soil. In the aquatic environment, material will sink and remain in the sediment.
Degradation and Persistence	This water insoluble polymeric solid is expected to be inert in the environment. Surface photodegradation is expected with exposure to sunlight. No appreciable biodegradation is expected.
Ecotoxicity	Not expected to be acutely toxic, but material may mechanically cause adverse effects if ingested by waterfowl or aquatic life.

13. DISPOSAL CONSIDERATIONS

DO NOT dump into any sewers, on the ground, or into any body of water. Disposal of wastes and used containers must be in accordance with applicable federal, state and local regulations. Regulations may vary in different locations. Waste characterizations and compliance with applicable laws are the responsibility solely of the waste generator. Stratasys Inc. has no control over the management practices or manufacturing processes of parties handling or using the material. The information presented here pertains only to the product as shipped in its intended condition as described in section two of this MSDS (Composition/Information on Ingredients).

14. TRANSPORT INFORMATION (NOT MEANT TO BE ALL-INCLUSIVE)

Department of Transportation (D.O.T.)	This product is not regulated by D.O.T. when shipped domestically by land
Canadian TDG Information	This product is not regulated by TDG when shipped domestically by land

STRATASYS®	**P400 ABS**
Material Safety Data Sheet	9/14/04

15. REGULATORY INFORMATION (NOT MEANT TO BE ALL-INCLUSIVE)

All components of this product are listed on these chemical inventories: U.S. TSCA, Canadian DSL, EU EINECS, Japanese ENCS, Korean ECL, Australian AICS.

U.S. Regulations

EPA SARA Title III Chemical Listings

This product has been reviewed according to the EPA "Hazard Categories" promulgated under Sections 311 and 312 of the Superfund Amendment and Reauthorization Act of 1986 (Sara Title III) and is considered under applicable definitions, to meet the following categories:
Not to have met any hazard category.

California Proposition 65

The following statement is made in order to comply with the California Safe Drinking Water and Toxic Enforcement Act of 1986:
Warning: This product contains a chemical(s) known to the State of California to cause cancer.

Toxic Substances Control Act (TSCA)

All ingredients are on the TSCA inventory and are not required to be listed on the TSCA inventory.

State Right-to-Know

This product is not known to contain any substances subject to the disclosure requirements of: New Jersey and Pennsylvania.

OSHA Hazard Communication Standard

This product is not a "Hazardous Chemical" as defined by the OSHA Hazard Communication Standard, 29 CFR 1910.1200.

Canadian Regulations

WHMIS Information: The Canadian Workplace Hazardous Materials Information System (WHMIS) Classification for this product is:
This product is not a "Controlled Product" under WHMIS.

STRATASYS®	**P400 ABS**
Material Safety Data Sheet	9/14/04

16. OTHER INFORMATION

THE INFORMATION contained in the PROCEEDING report is based upon current knowledge, our experience with the product, and is not exhaustive. While not guaranteed, the information presented herein was prepared by a competent, technical professional and is true and accurate to the best of our knowledge. The information applies to product as defined by the specifications. If the product is mixed with other substances, the customer must confirm that no new hazards exist. In all cases, the user is not exempt from following all legal, administrative and regulatory procedures relating to the product, personal hygiene, and the integrity of the work environment. Stratasys Inc. shall not be held liable for any damage resulting from handling or from contact and use with the above product.

Revision History

Revision	Revision Date
1.0	11/97
1.1	3/15/04
1.2	4/14/04
1.3	9/14/04